ESA - MOST Dragon 2 Programme
2011 DRAGON 2 SYMPOSIUM

中国科技部-欧洲空间局合作 "龙计划"二期
"龙计划"二期2011年学术研讨会

InSAR Error Analysis in Monitoring Coseismic Deformation of 2008 Damxung M_w 6.3 Earthquake

Zhang Jingfa, Liu Bin, Luo Yi and Zeng Qiming

Institute of Crustal Dynamics, China Earthquake Administration
100085, Beijing, China
Institute of GIS and RS , Peking University
Beijing, China

OUTLINE

- Geological & Seismological Features
- Error Analysis & Deformation
- Numerical Simulation
- Conclusions

Geological & Seismological Features

October 6, 2008, The Mw6.3 earthquake occurred in Damxung area of the Tibetan Plateau, located at 90.3E, 29.8N (CENC). Depth 8.0 km.

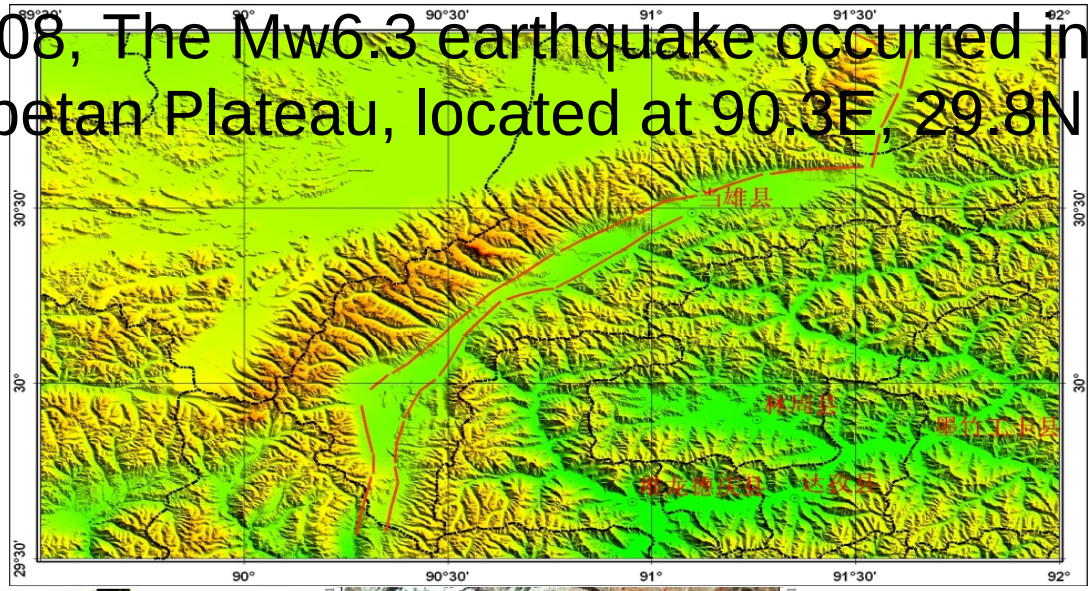

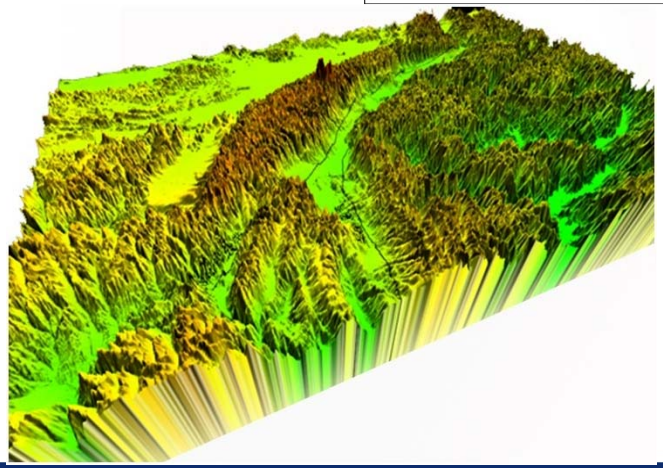

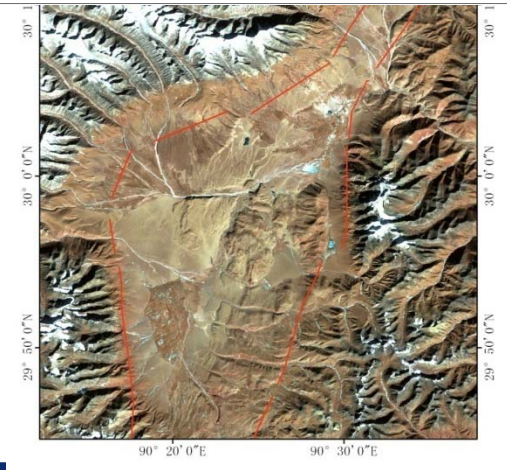

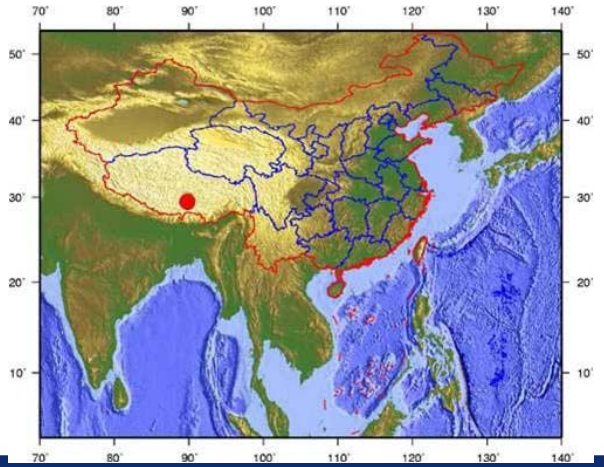

Geological & Seismological Features

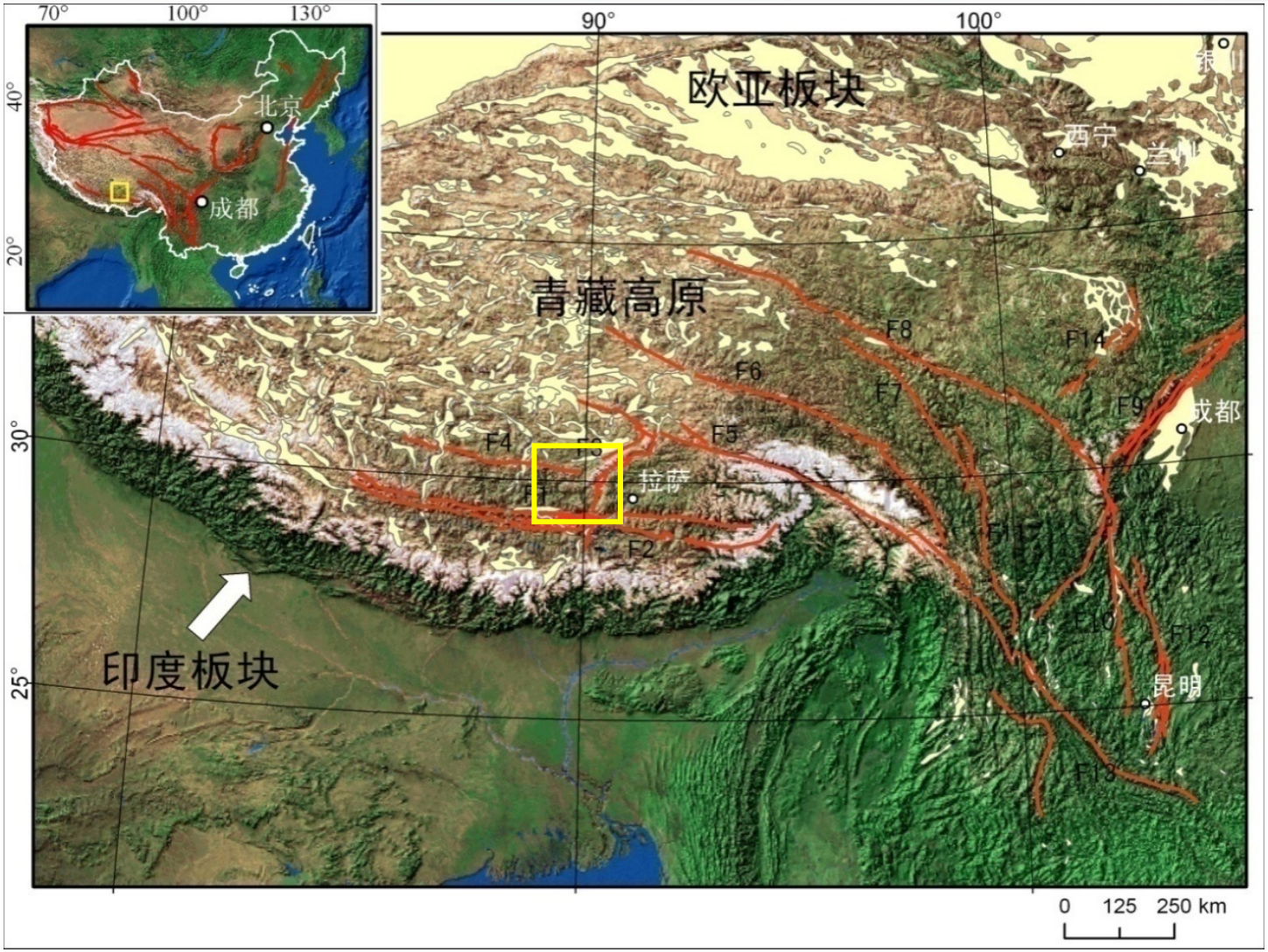

Geological & Seismological Features

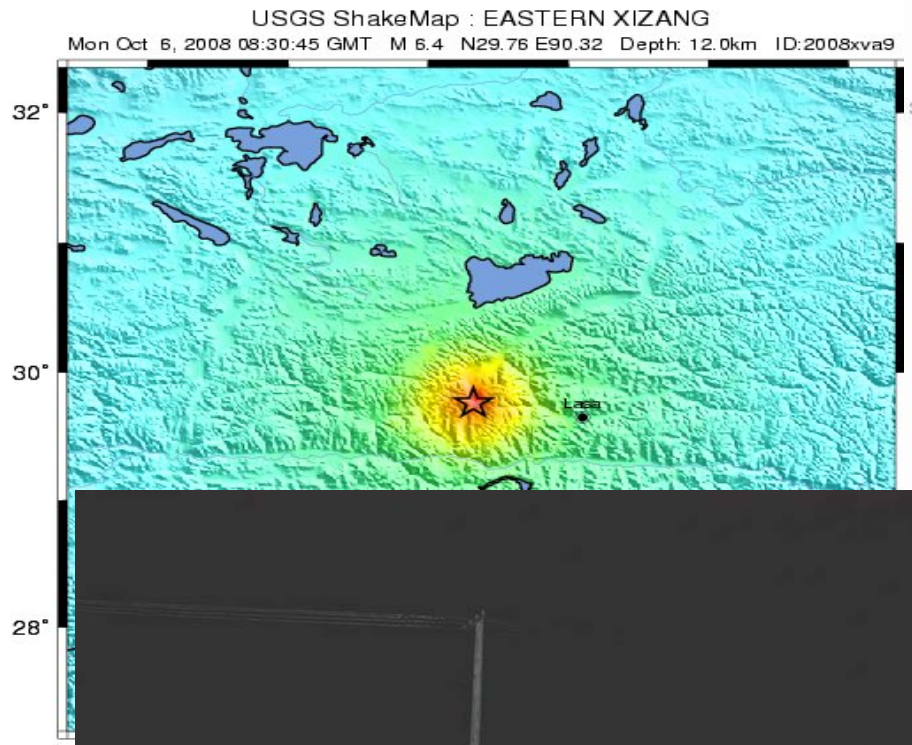

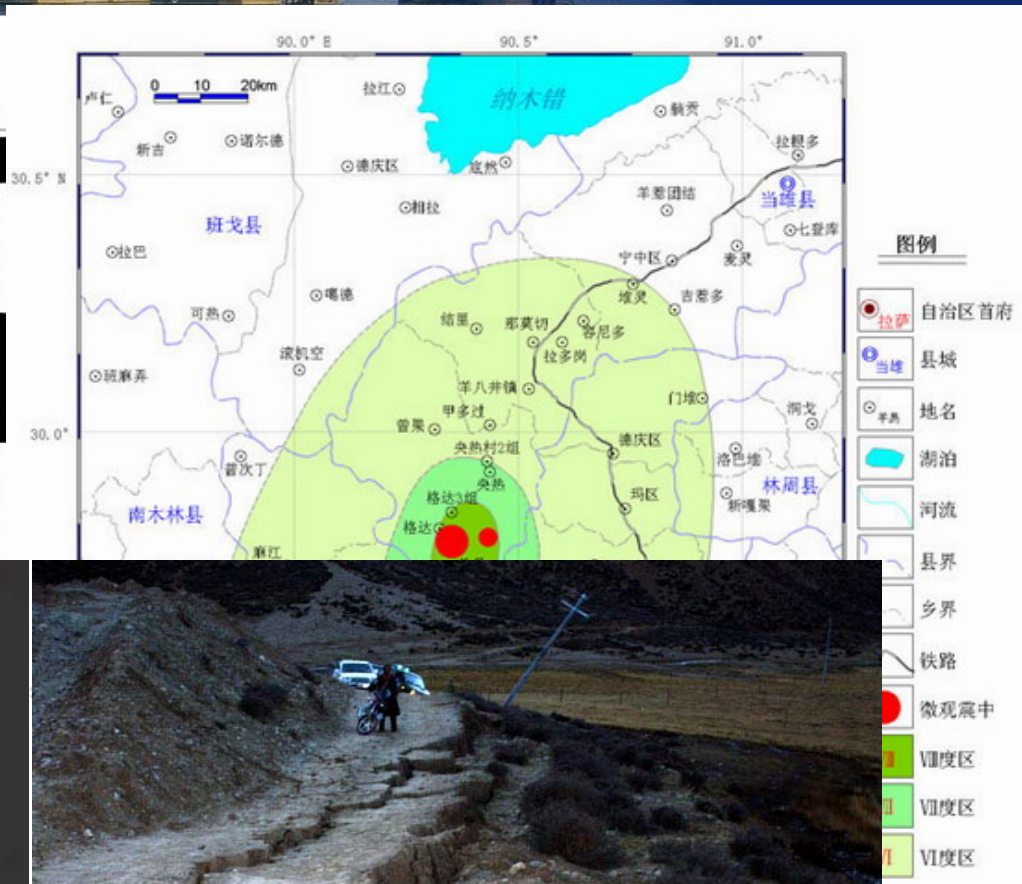

Geological & Seismological Features

Epicenter distribution map from 1970 to 2008

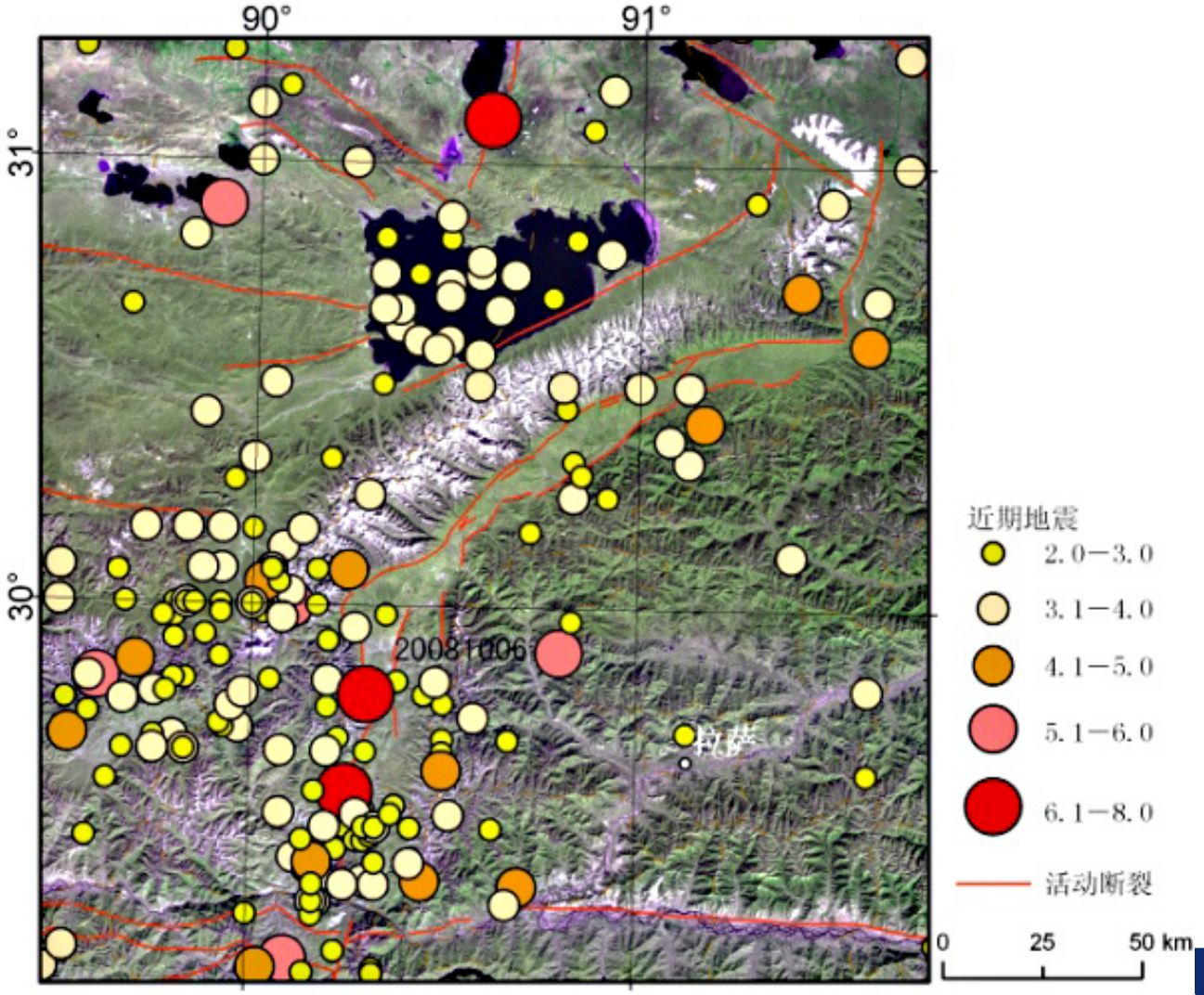

Geological & Seismological Features

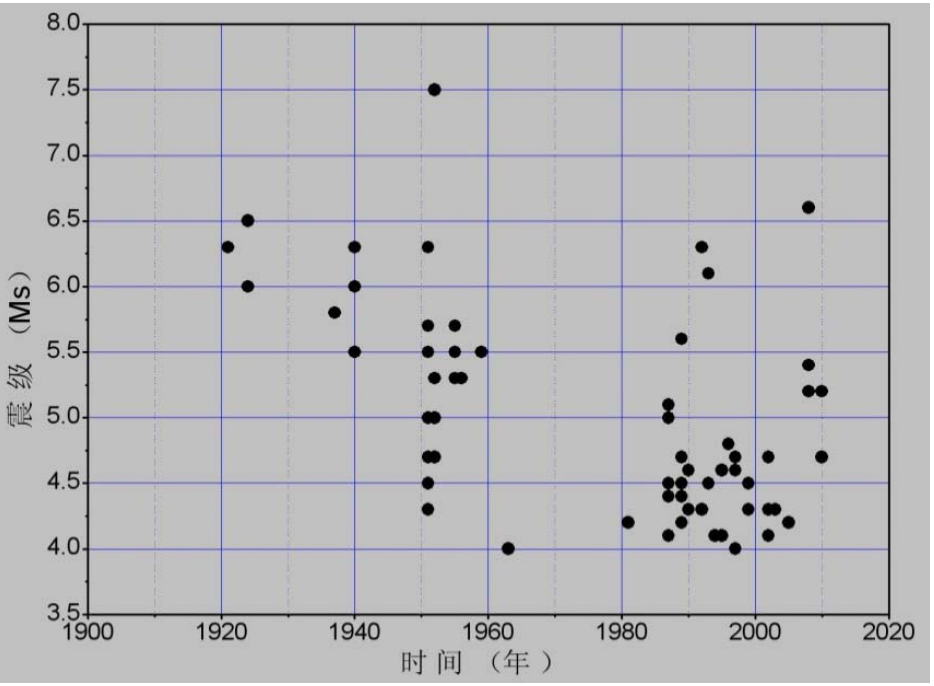

Ms≥4.0 earthquakes Ms-Time image in Damxung

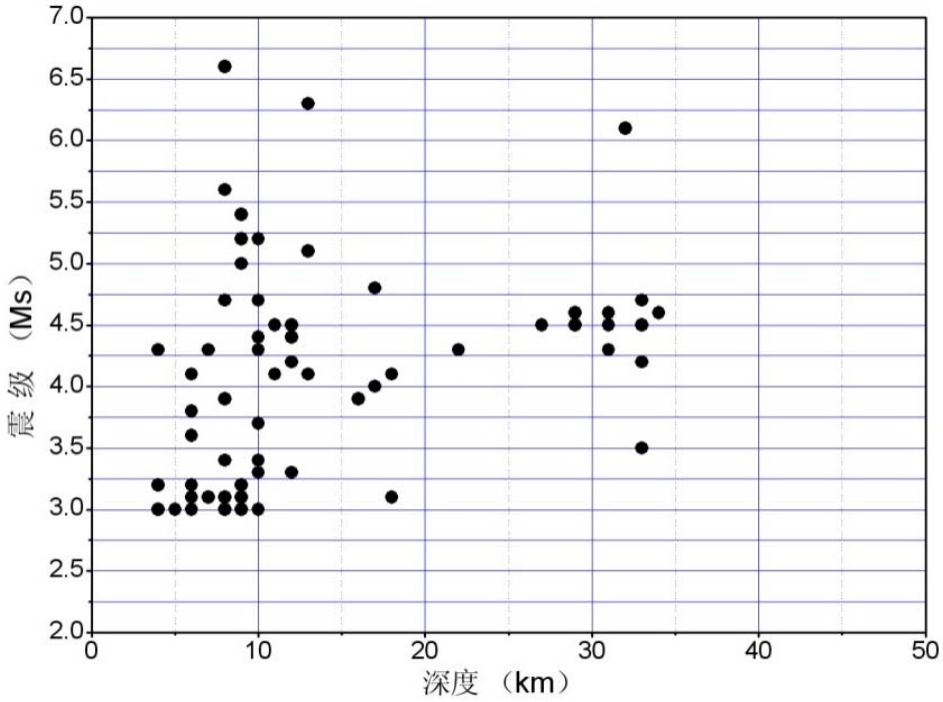

Ms≥4.0 earthquakes Ms-Depth image in Damxung

OUTLINE

- Geological & Seismological Features
- Error Analysis & Deformation
- Numerical Simulation
- Conclusions

Results of different incidence angles

Descending paths

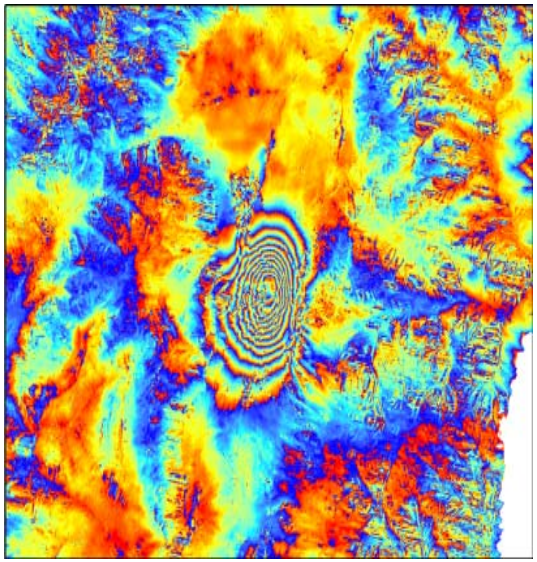

Strip T176

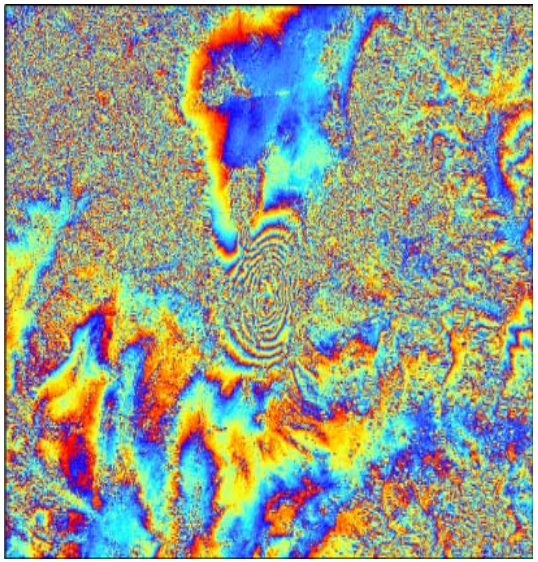

WS T362

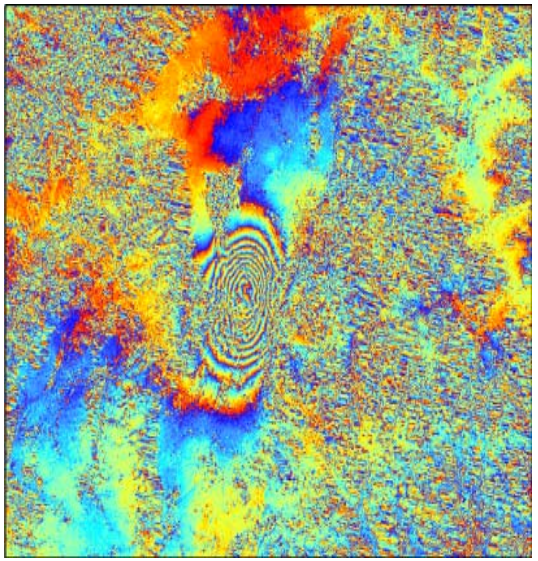

WS T405

Results of different incidence angles

Descending paths

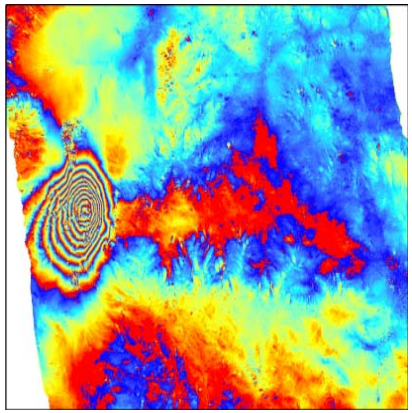

Strip T26

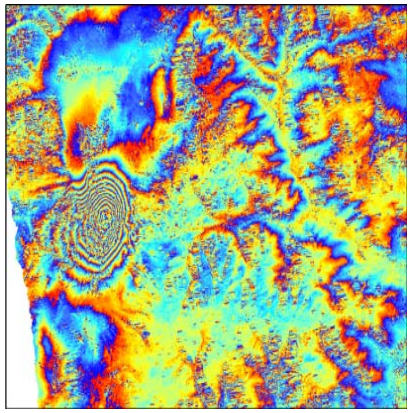

WS T212

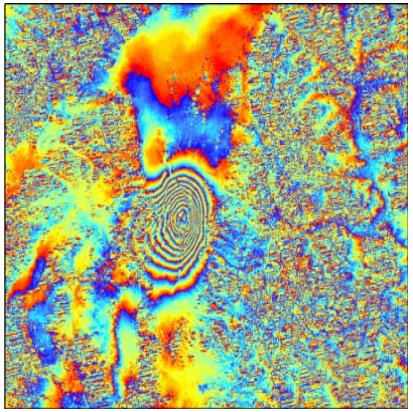

WS T441 HH-HH

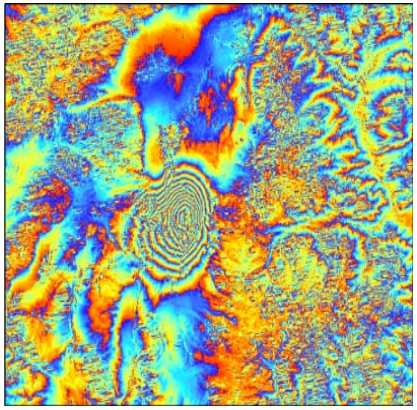

WS T441 HH-VV

InSAR results of different incidence angles and polarization show the deformation characteristics of Damxung earthquake.

Registration of Master & Slave

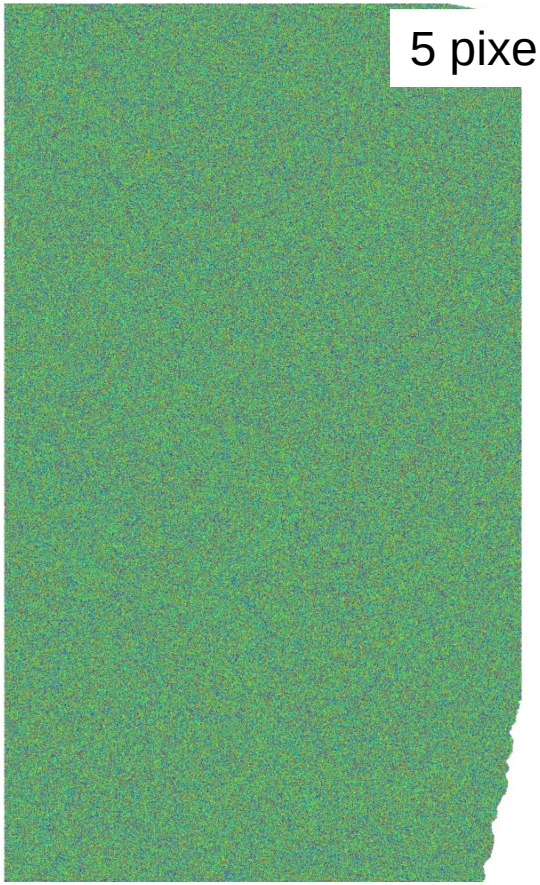

5 pixel deviation

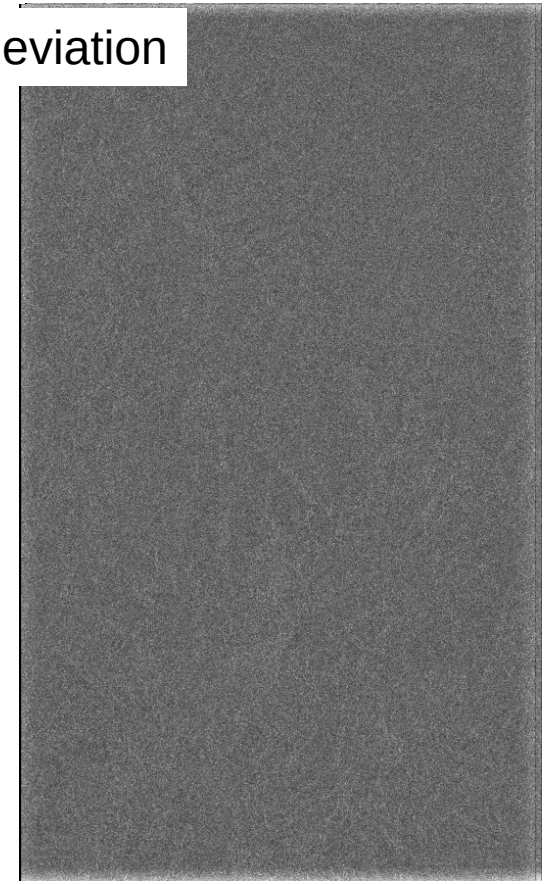

Interferogram

Coherence

Registration of Master & Slave

The relations between coherence and pixel deviations

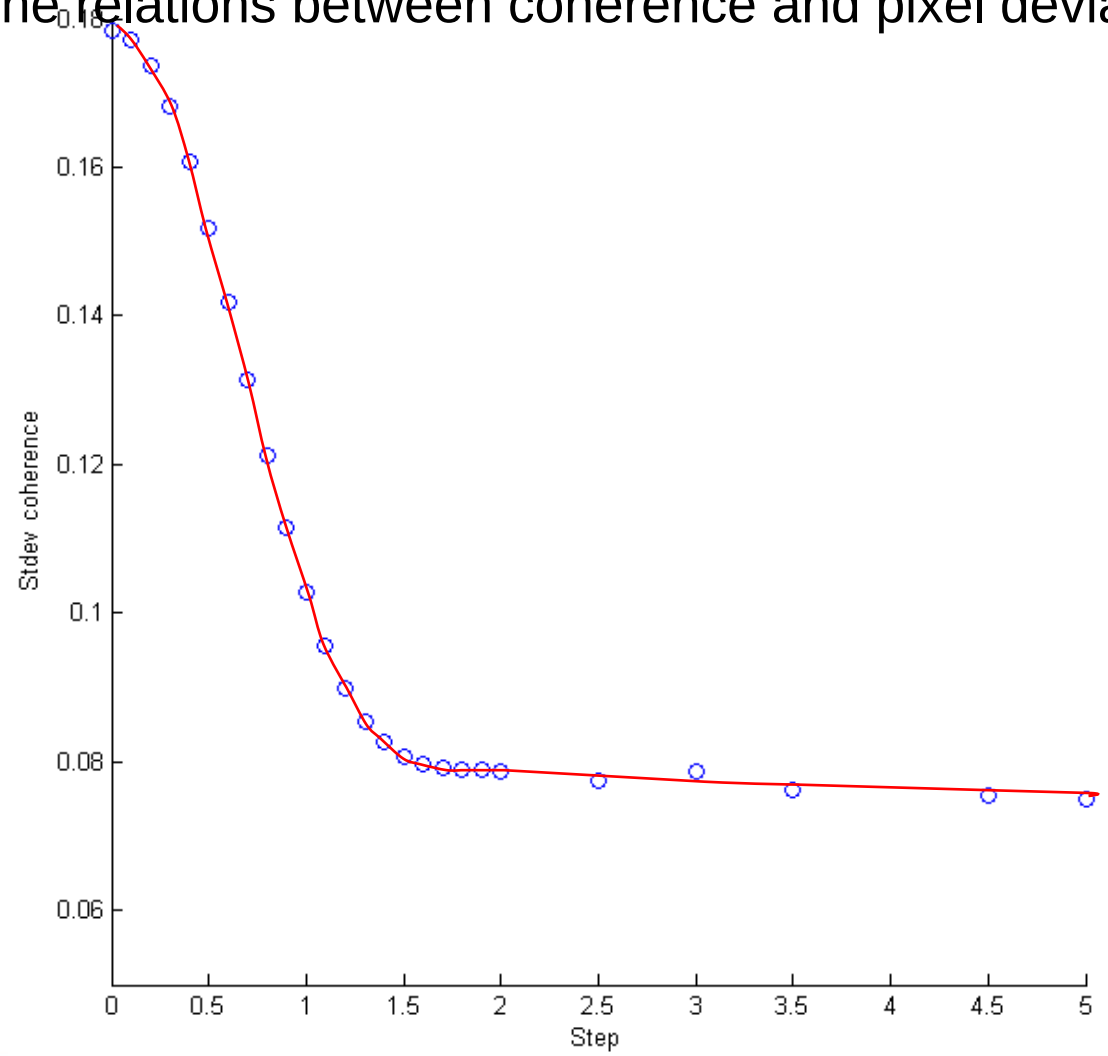

Registration of Master & DEM

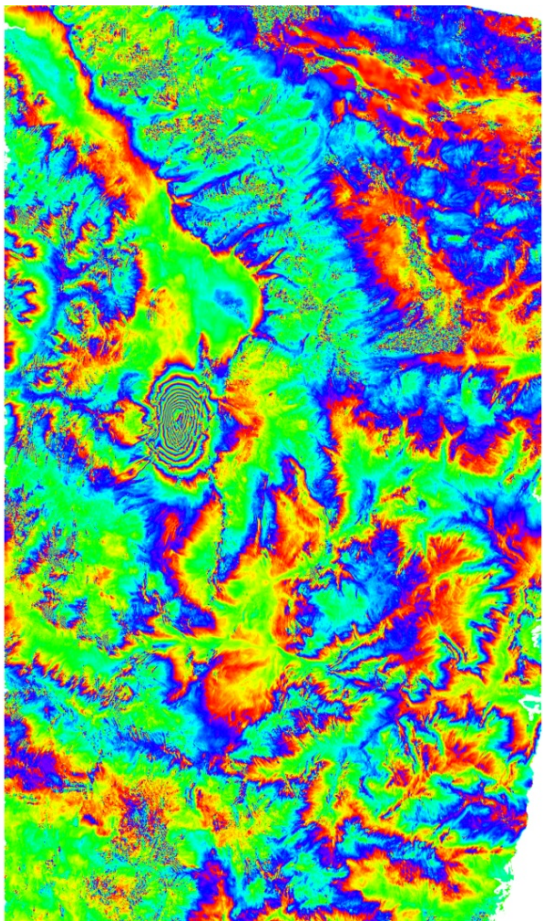

Original images

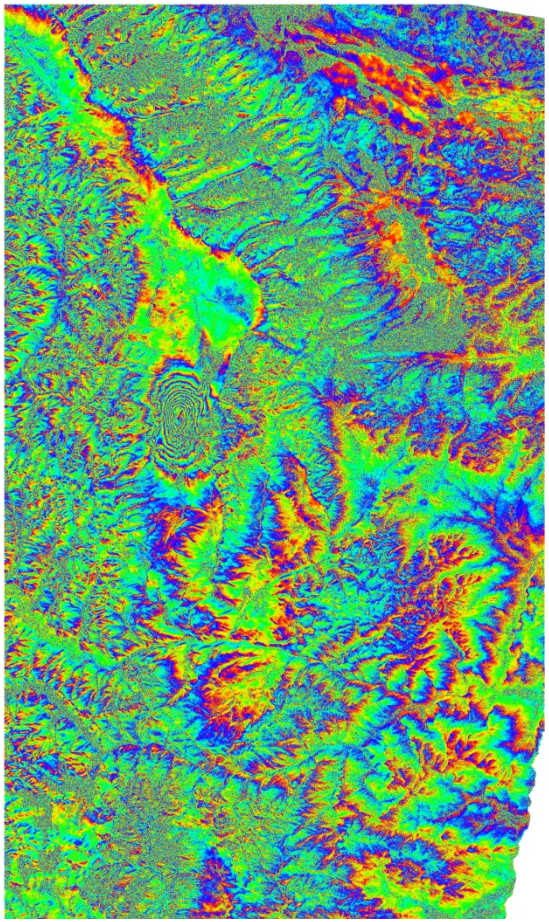

5 pixels deviation

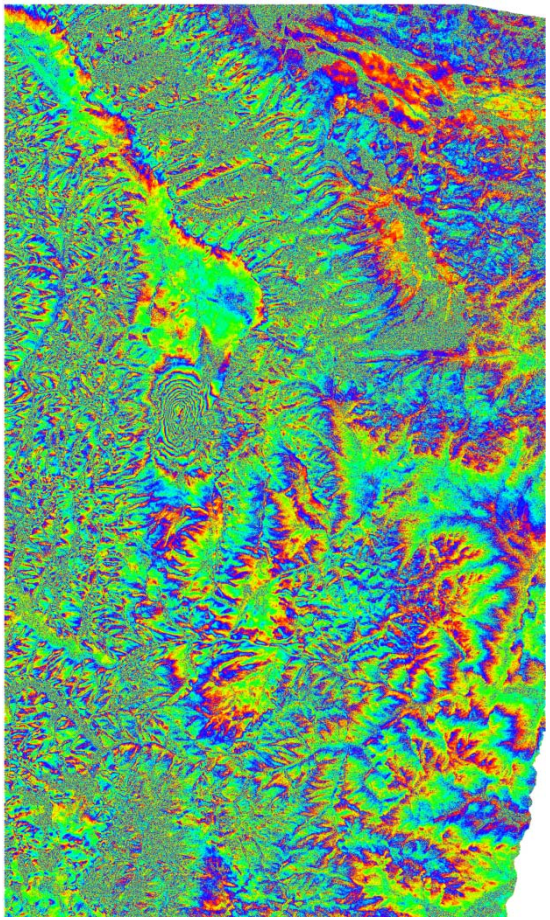

10 pixels deviation

Comparison of different unwrapping methods

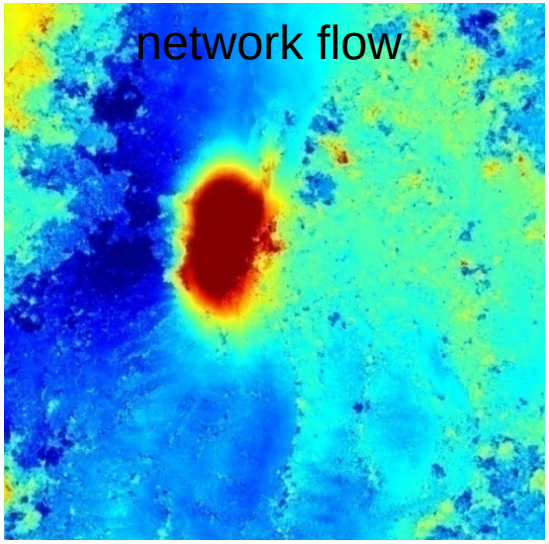

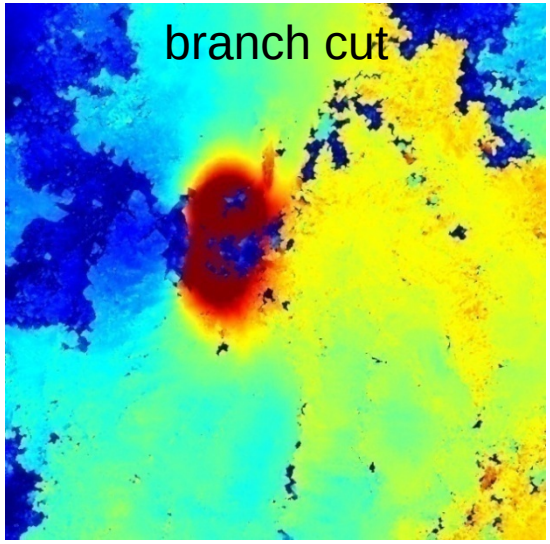

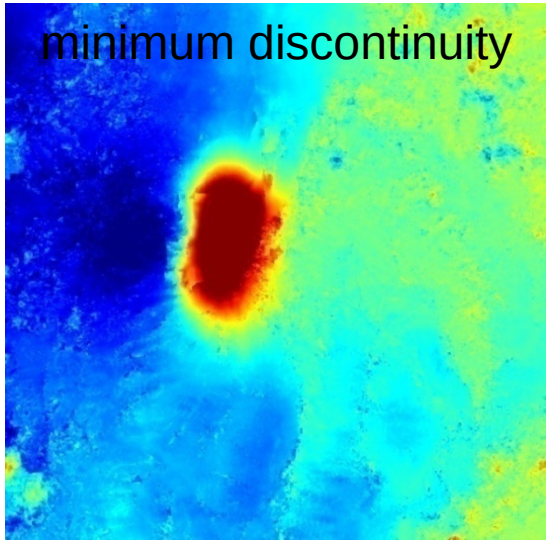

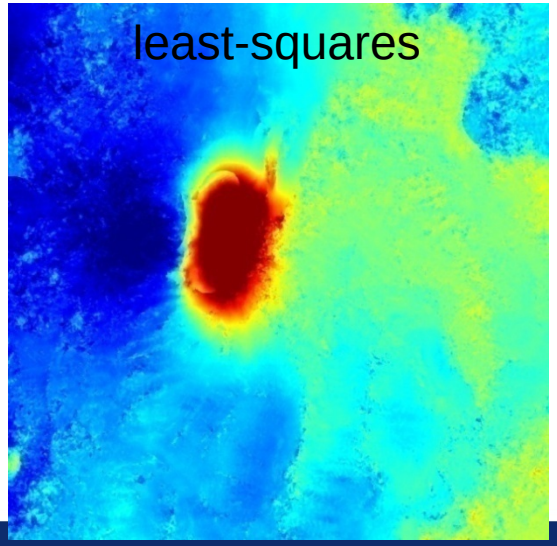

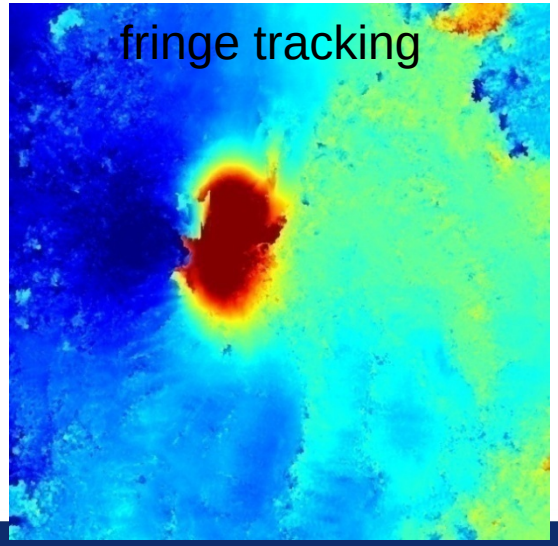

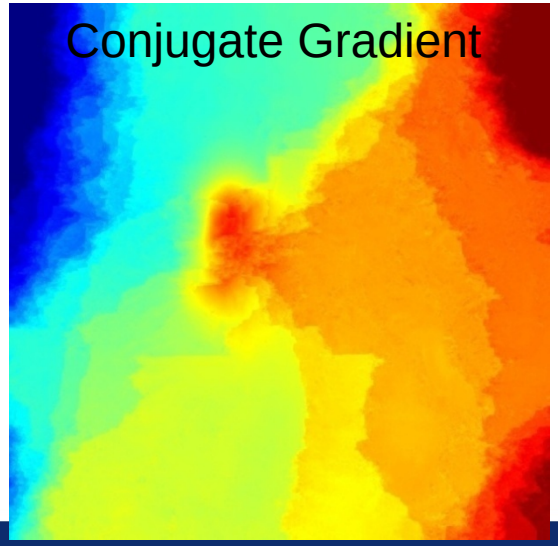

Comparison of different unwrapping methods

comparative analysis of different unwraped methods

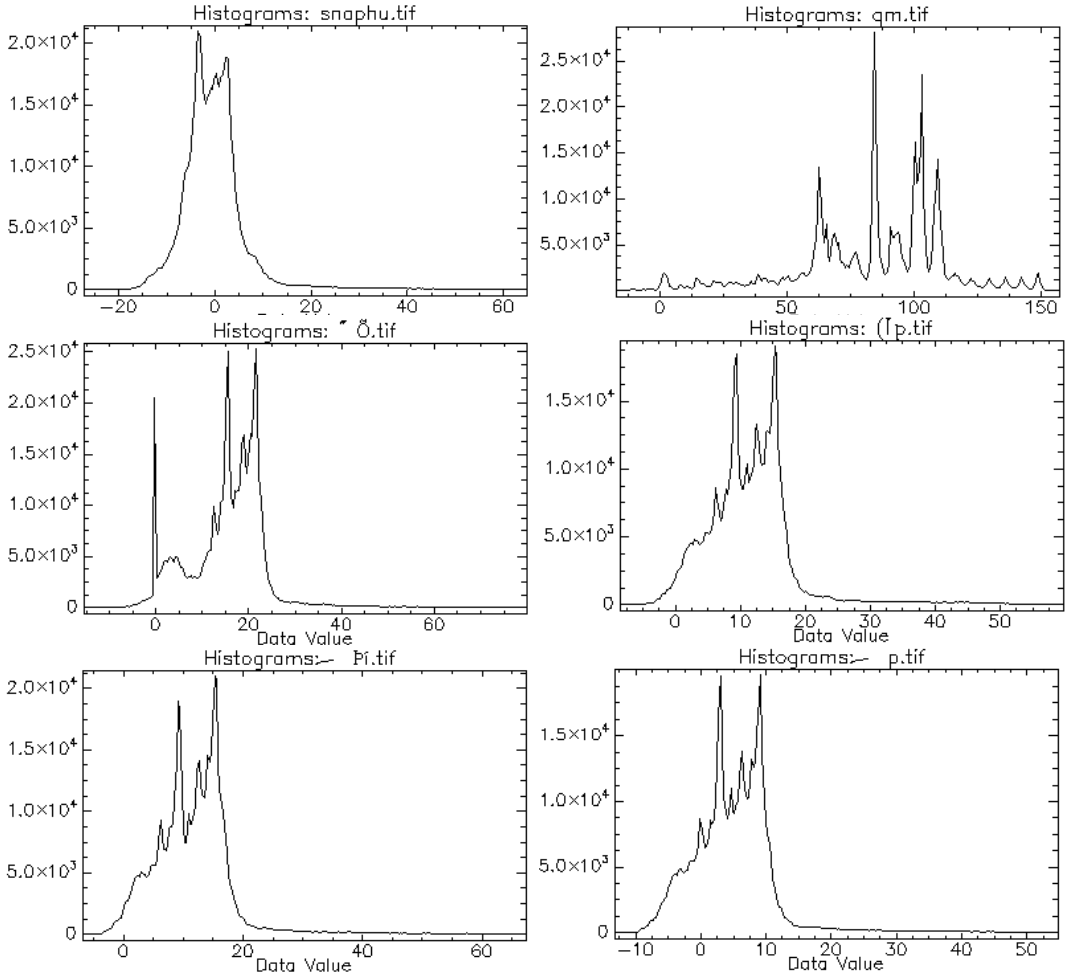

Unwrapping errors detection

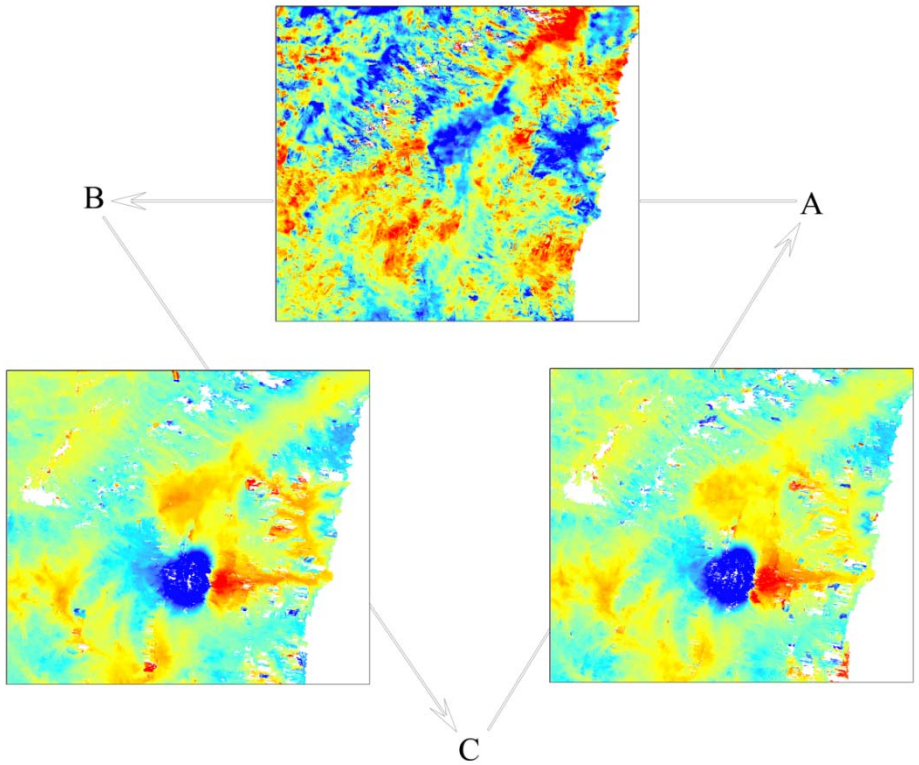

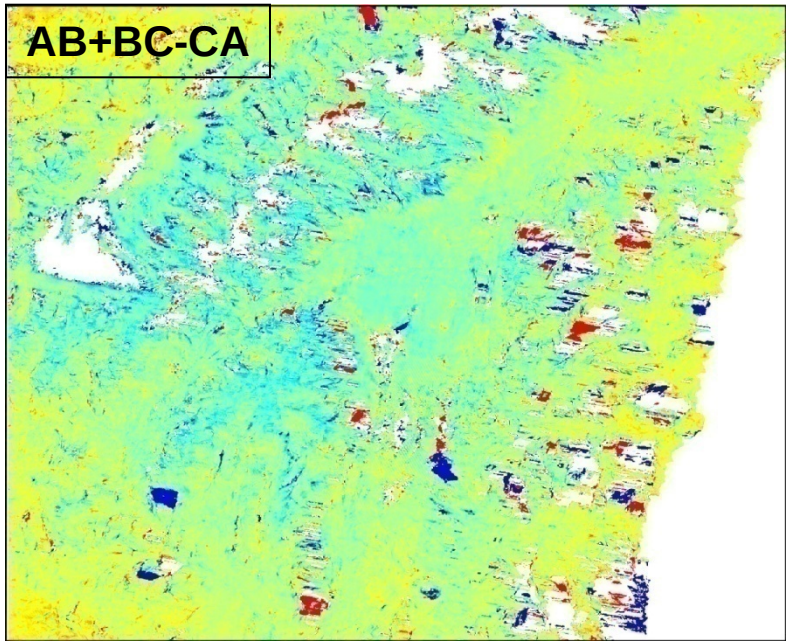

T441,WS A: 20080731, HH;
B: 20081009, HH; C: 20081218, VV

Mean：0.1932；
Standard Deviation：1.2271

Topography correct atmospheric path delays

Atmospheric path delays caused by topography

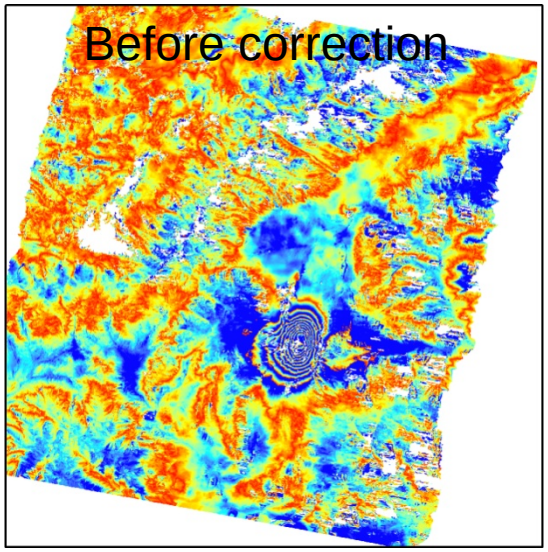

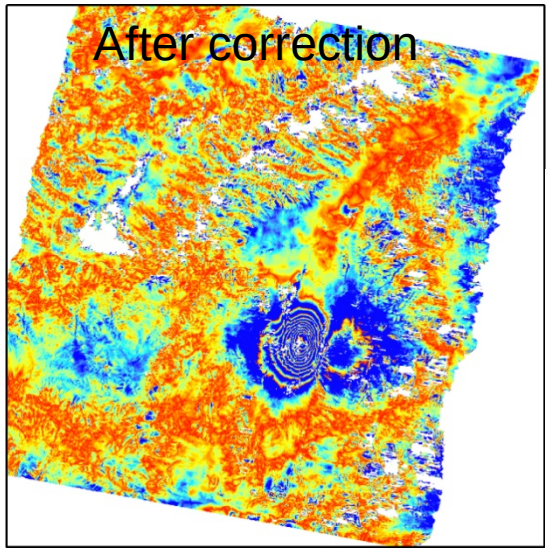

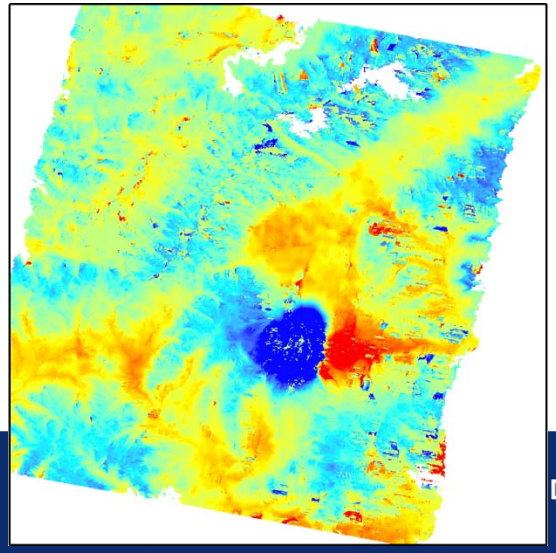

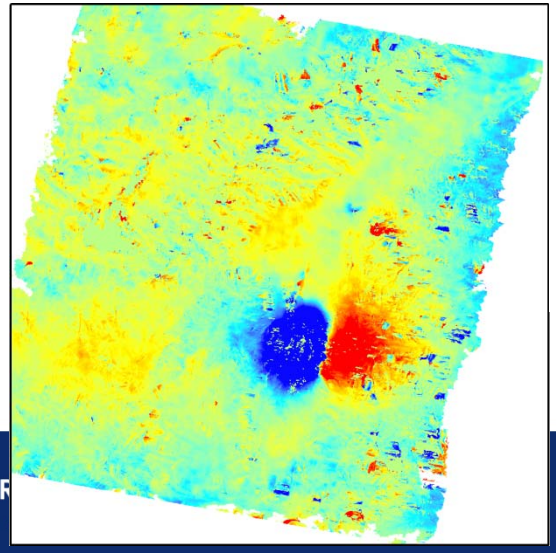

Descending path:
T176

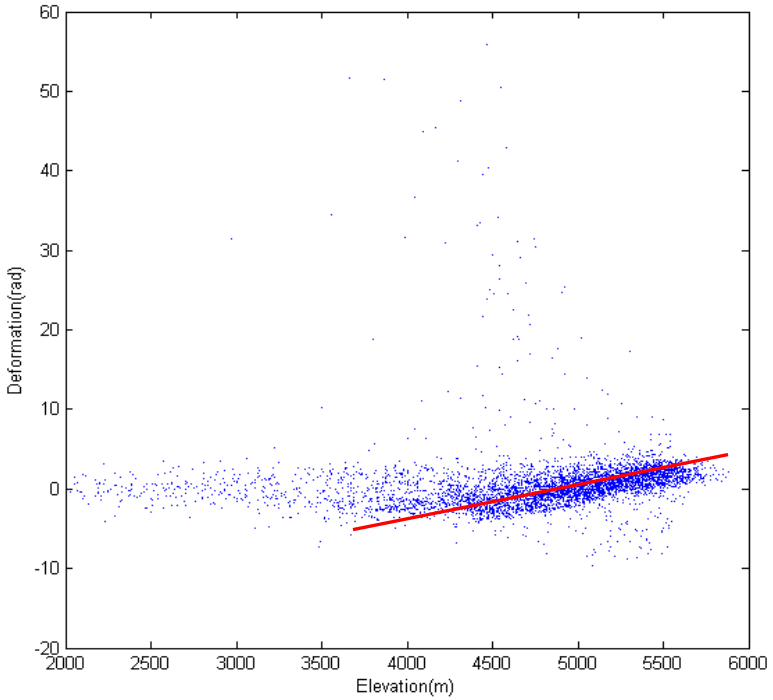

Topography correct atmospheric path delays

Befo

ction

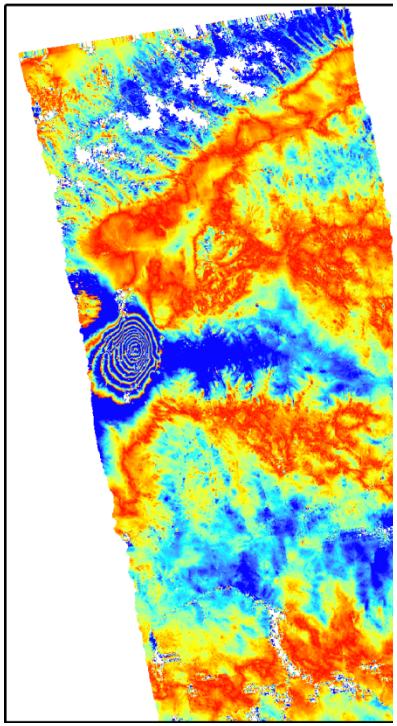

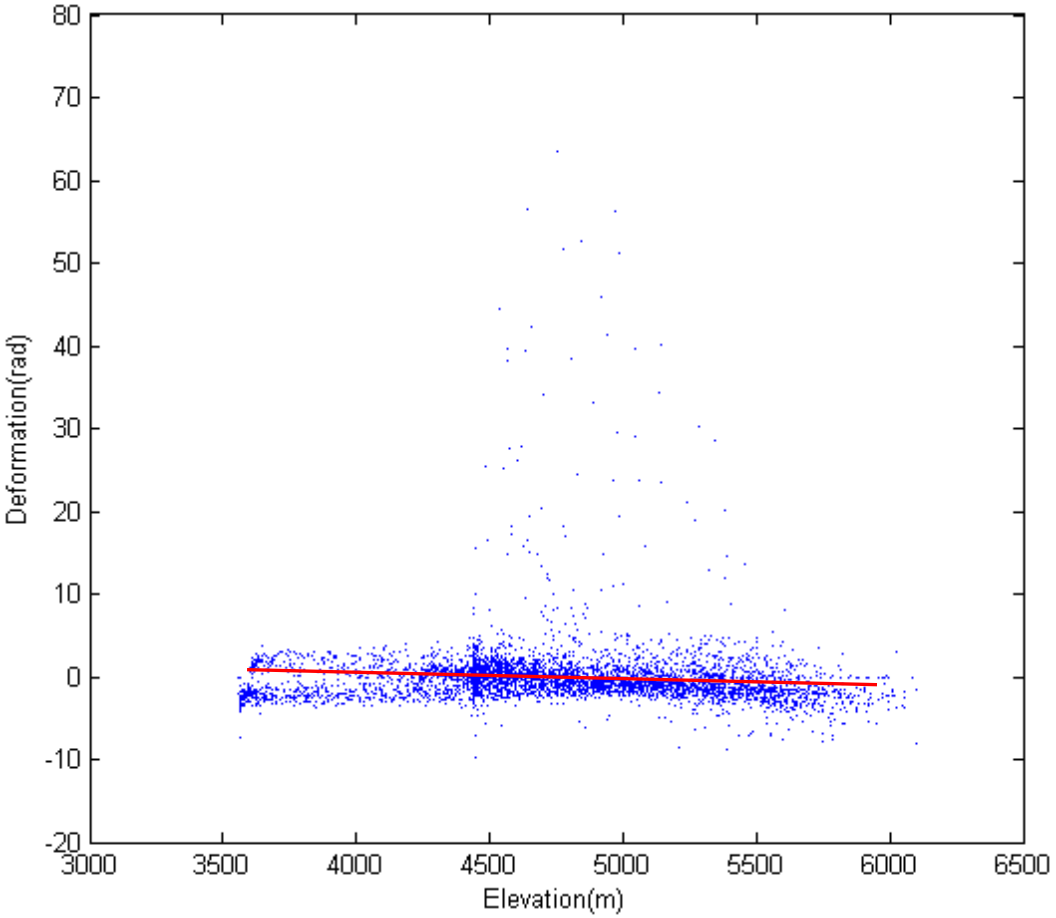

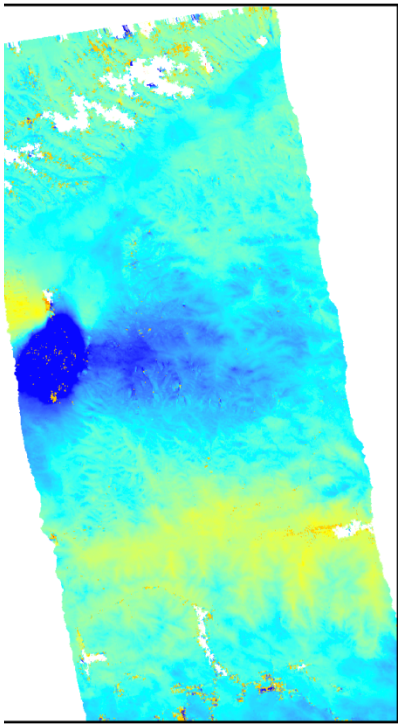

Topography correct atmospheric path delays

Atmospheric path delays caused by topography

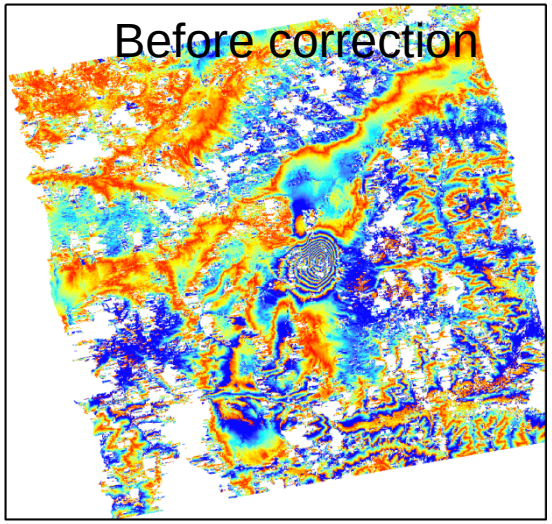

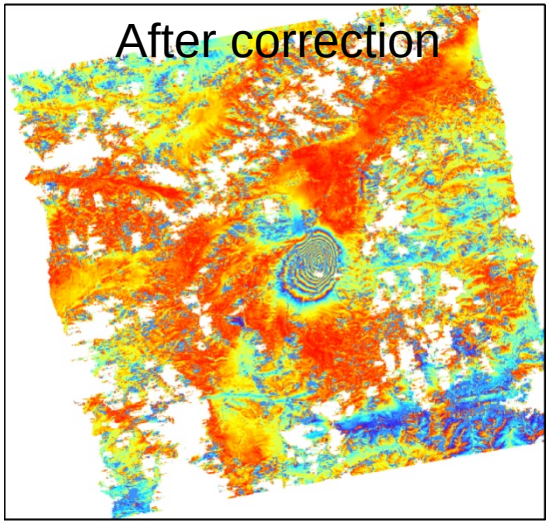

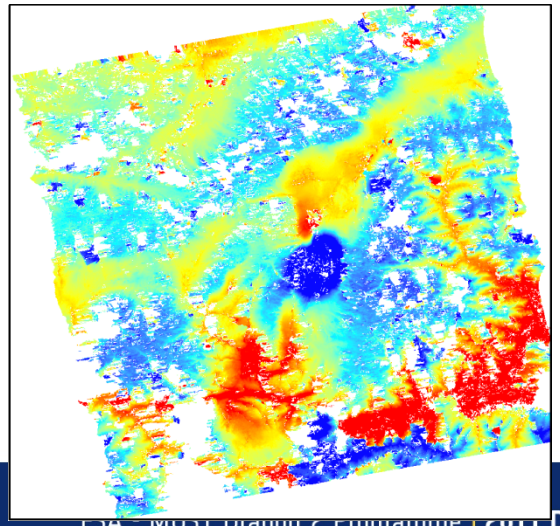

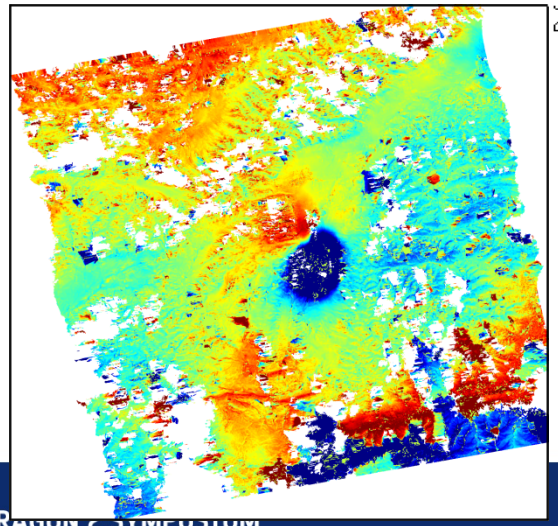

Ascending path:
WS T441 H/V

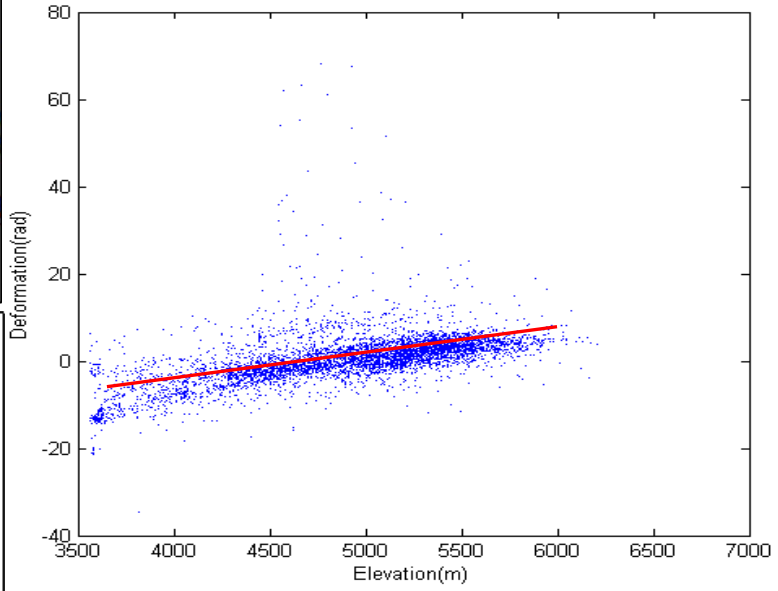

Effects of baseline refinement

The deformation signal is small in the interferogram, and it is possible to define a ‘far-field’ area of the interferogram which is not affected by deformation and use this to re-estimate the baseline parameters. However, the deformation signal covers such a large area that there is no true ‘far-field’ (Biggs et al, 2007), Such as Yushu, Manyi earthquake, in these cases, this baseline refined procedure should be more careful!!!

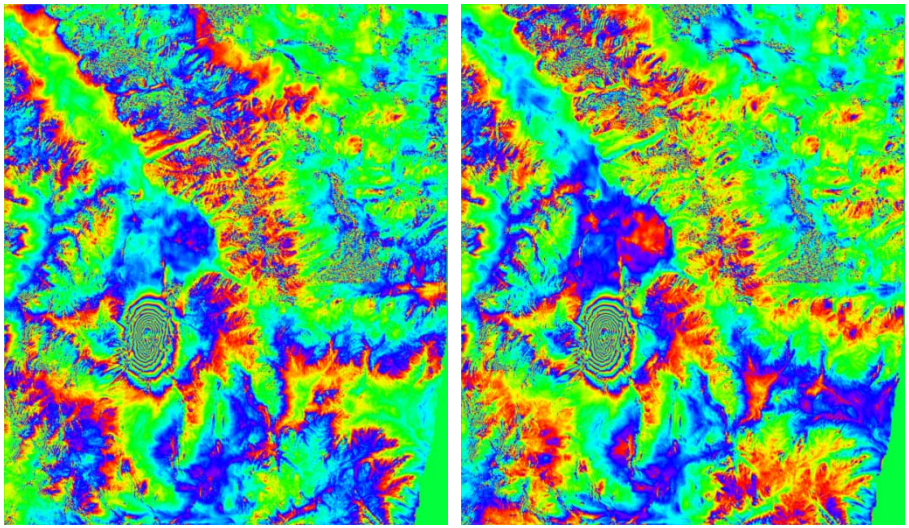

T176

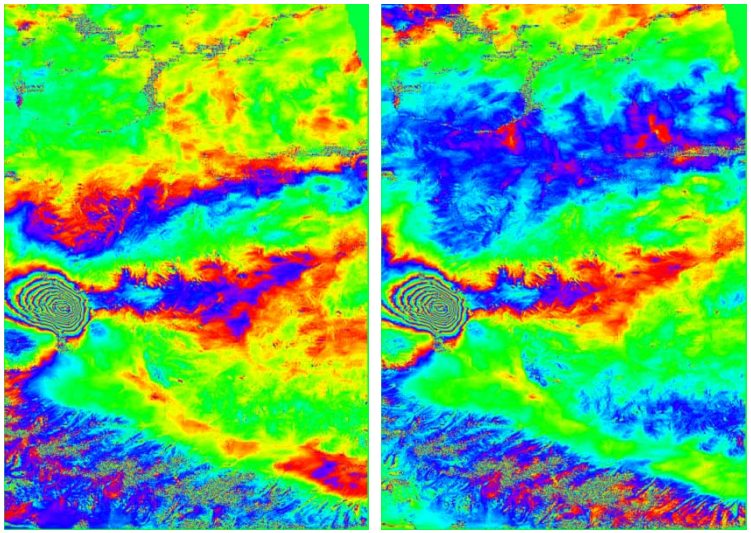

T26

Effects of baseline refinement

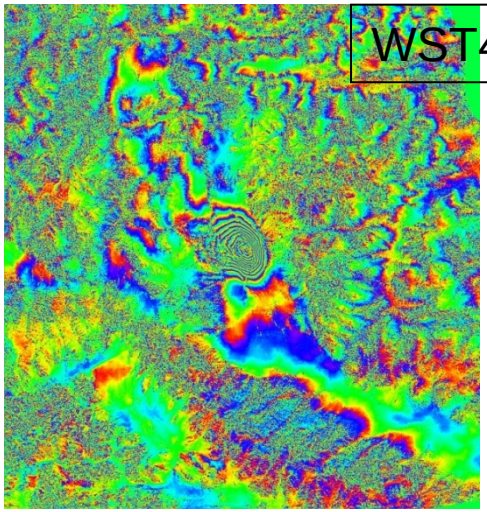

WST441 HH

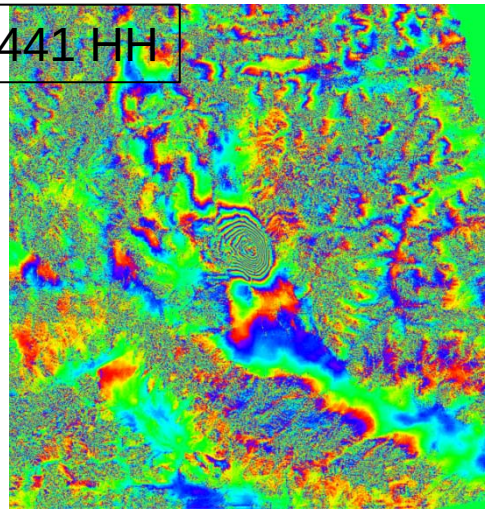

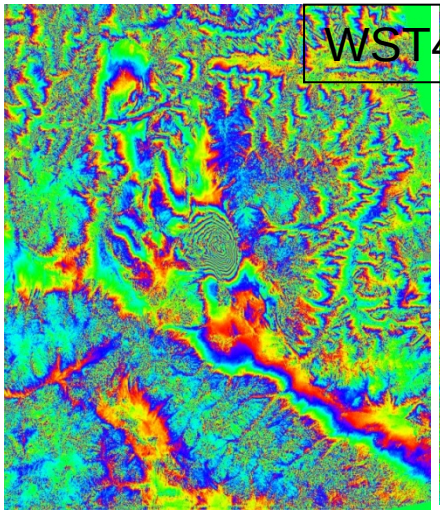

WST441 HV

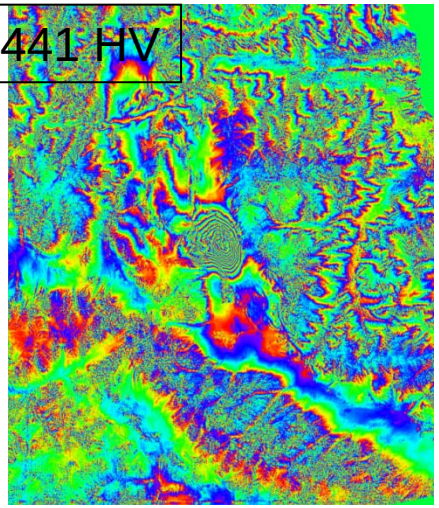

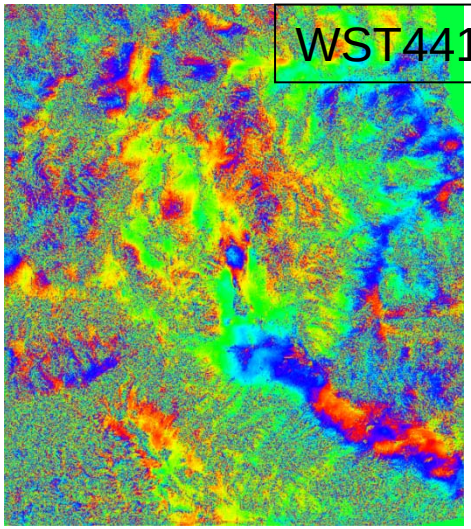

WST441 HV pos

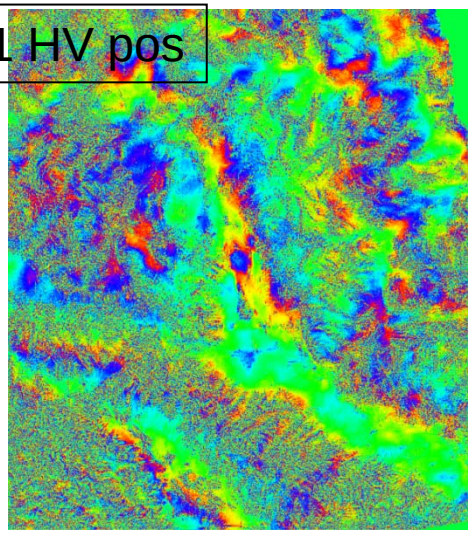

Time series analysis for Dumxiong Fault By using PS & SBAS

Before the Earthquake, T176, 34 ASAR images collected

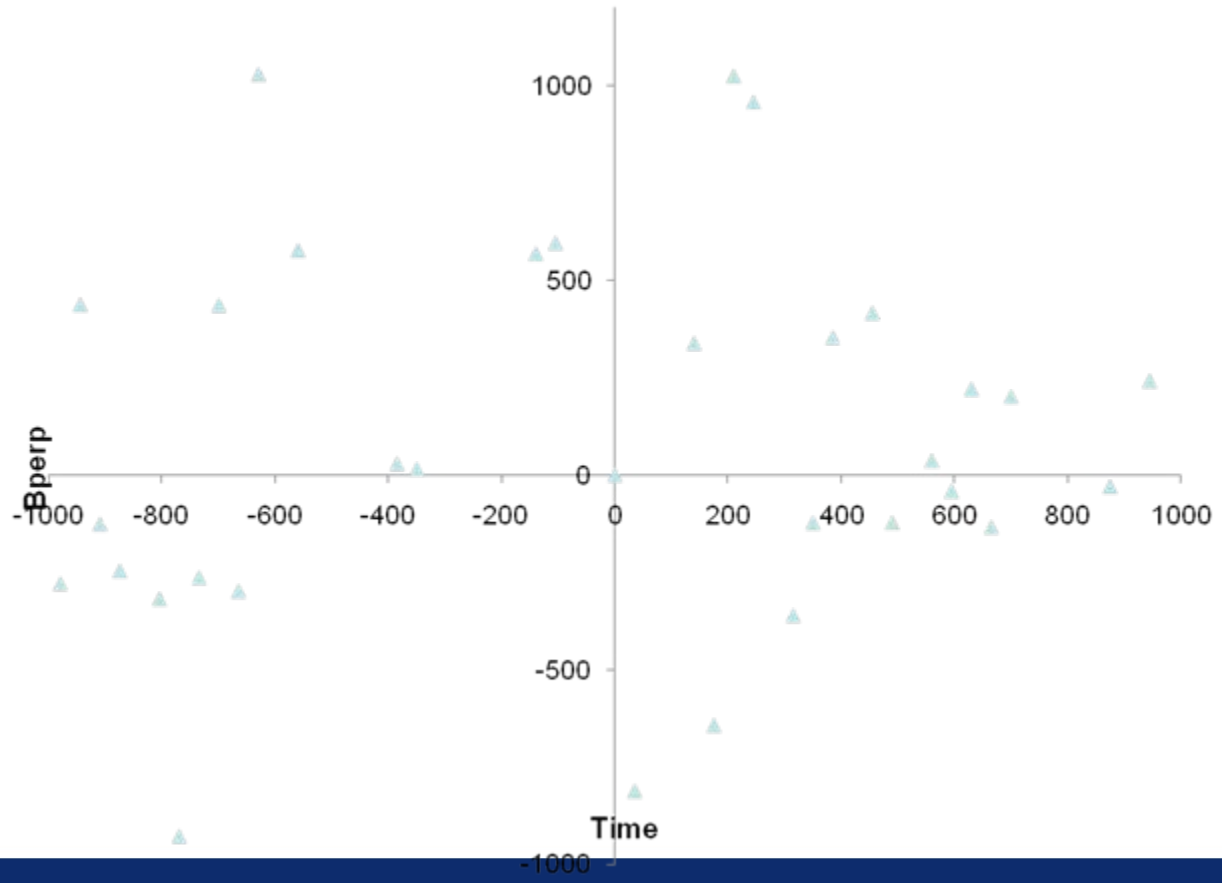

PS InSAR baseline

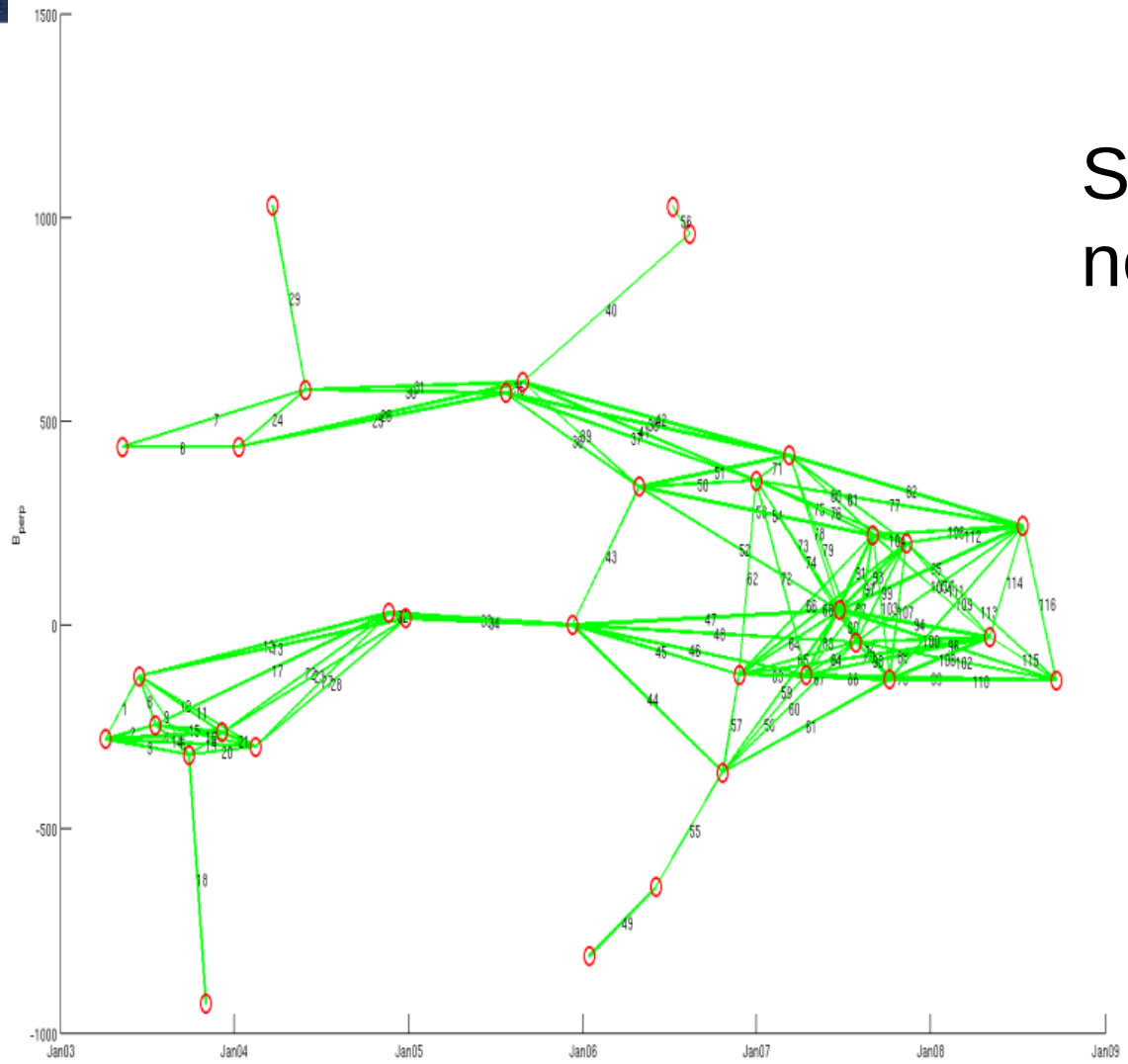

SBAS interferometric network

Time series analysis before the earthquake

Unwraped images of PS points

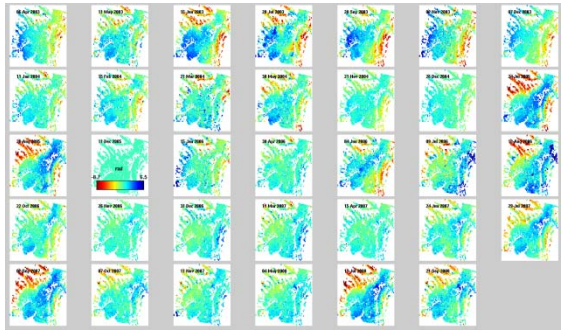

Orbital contribution

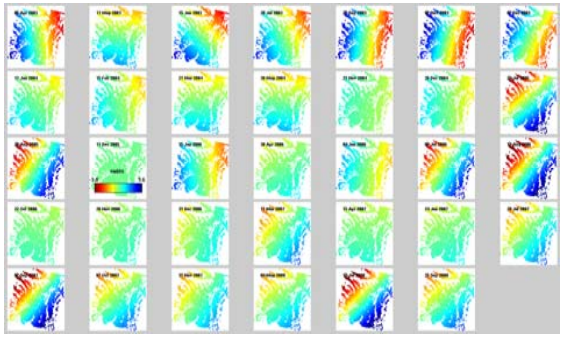

Atmospheric contribution

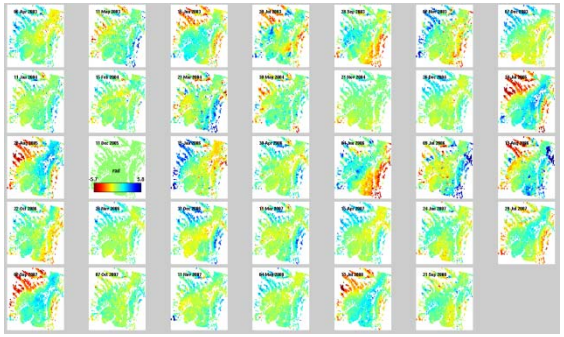

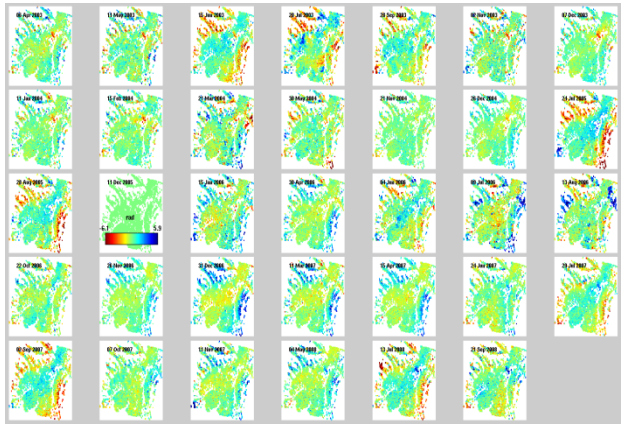

DEM error

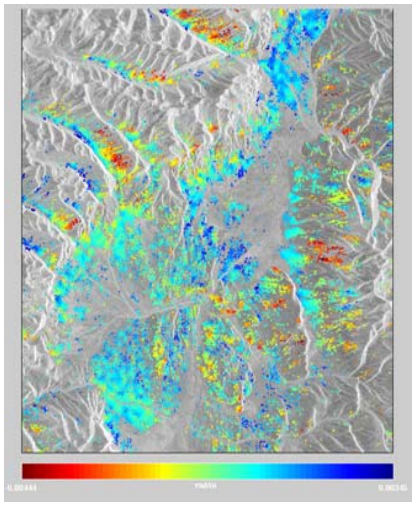

Time series of deformation signal

Time series analysis before the earthquake

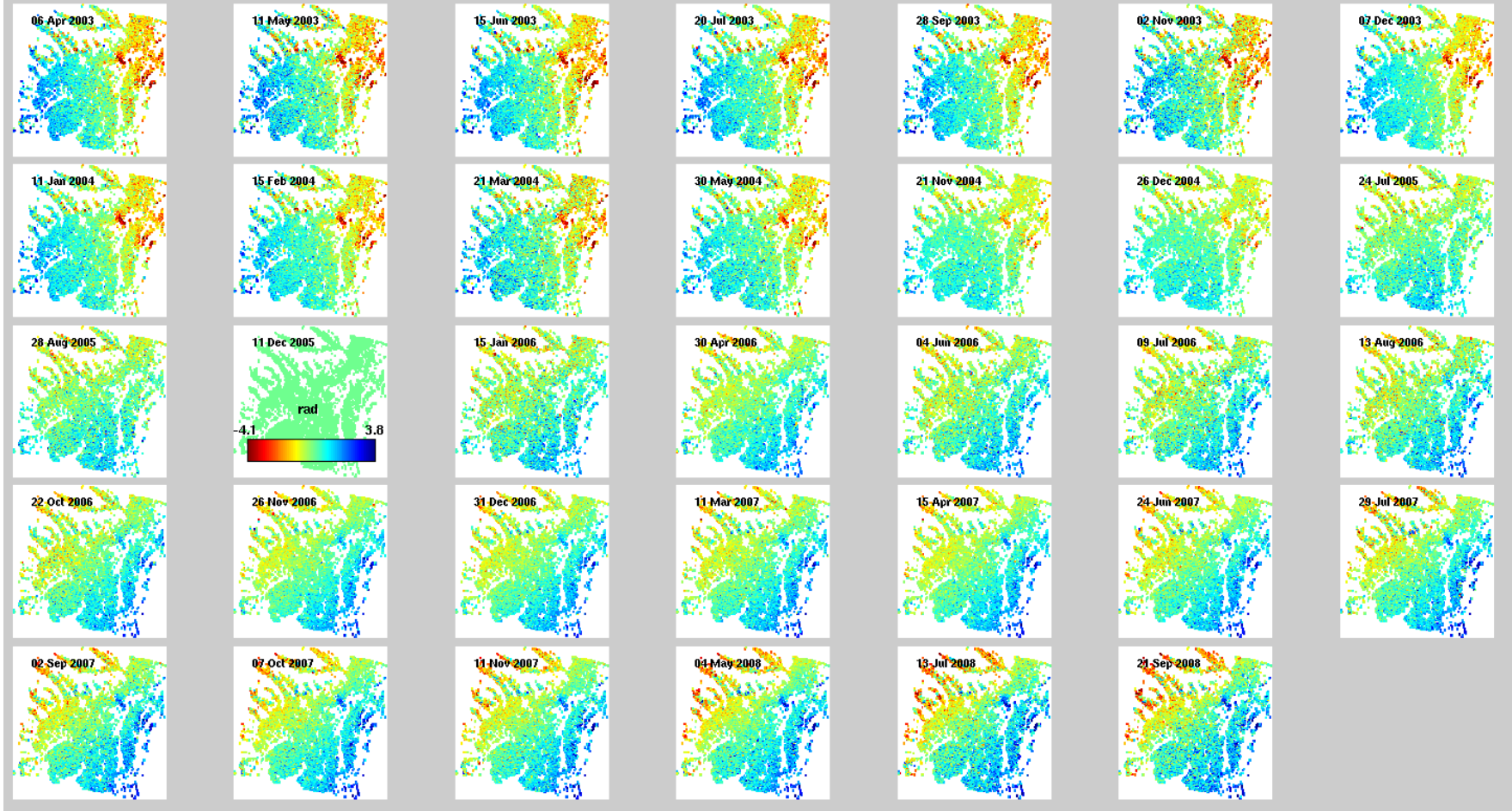

Time series analysis before the earthquake

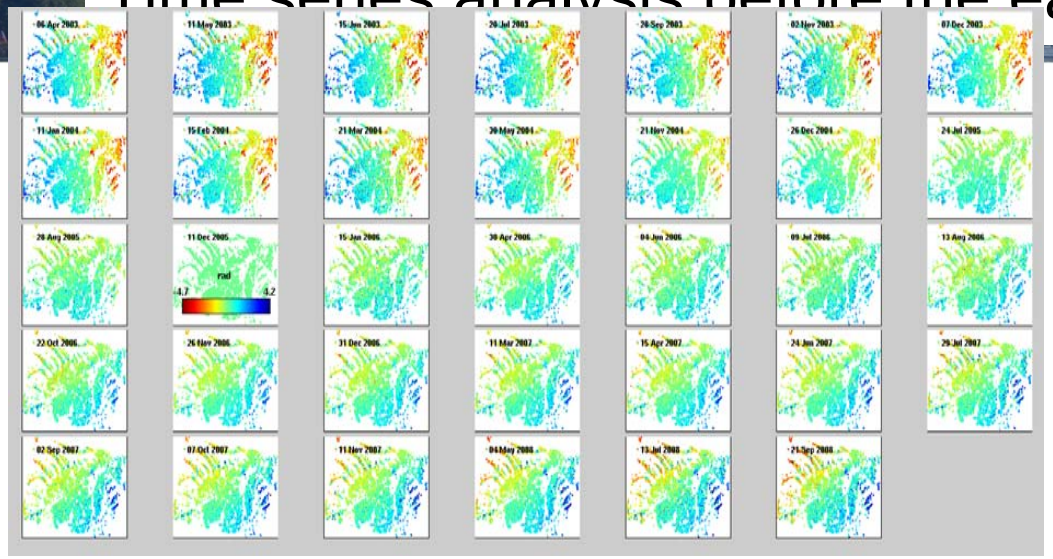

PS-InSAR Time series of deformation signals

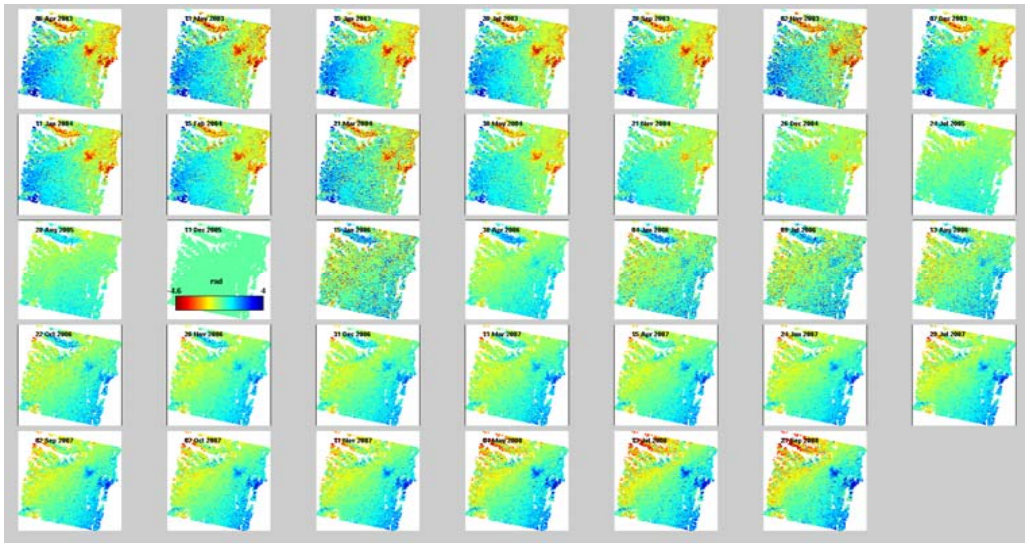

SBAS-InSAR Time series of deformation signals

Time series analysis before the earthquake

PS InSAR

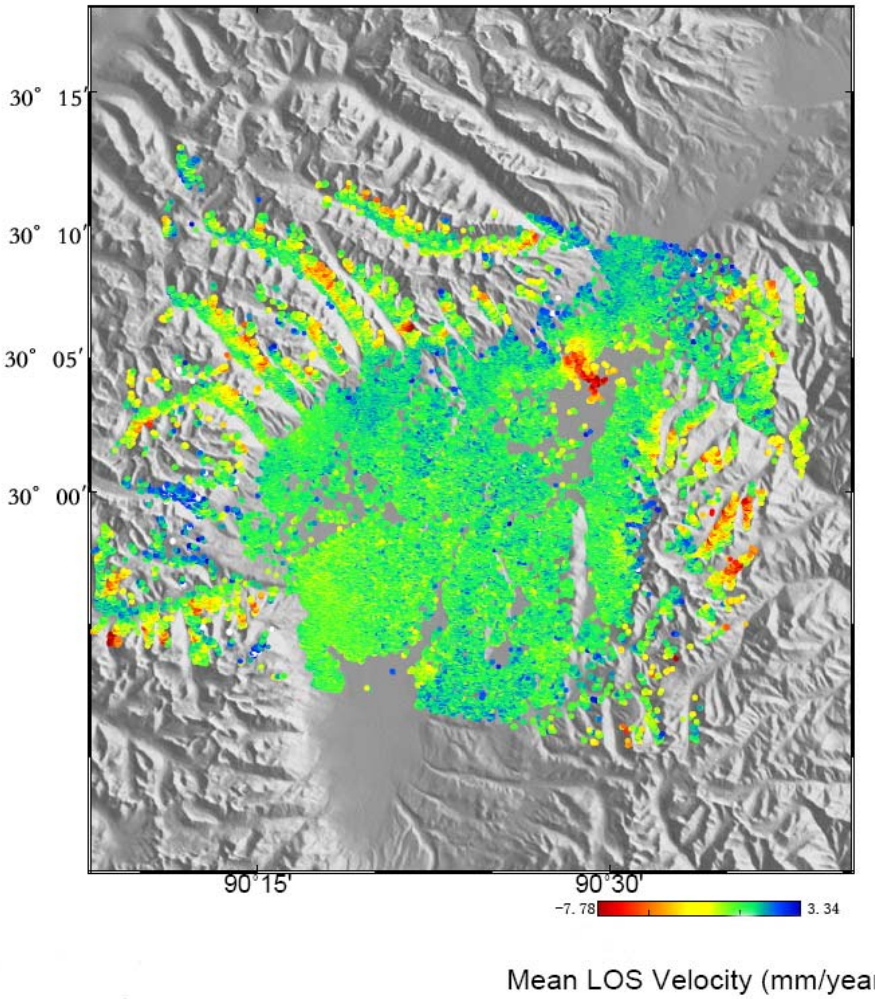

SBAS InSAR

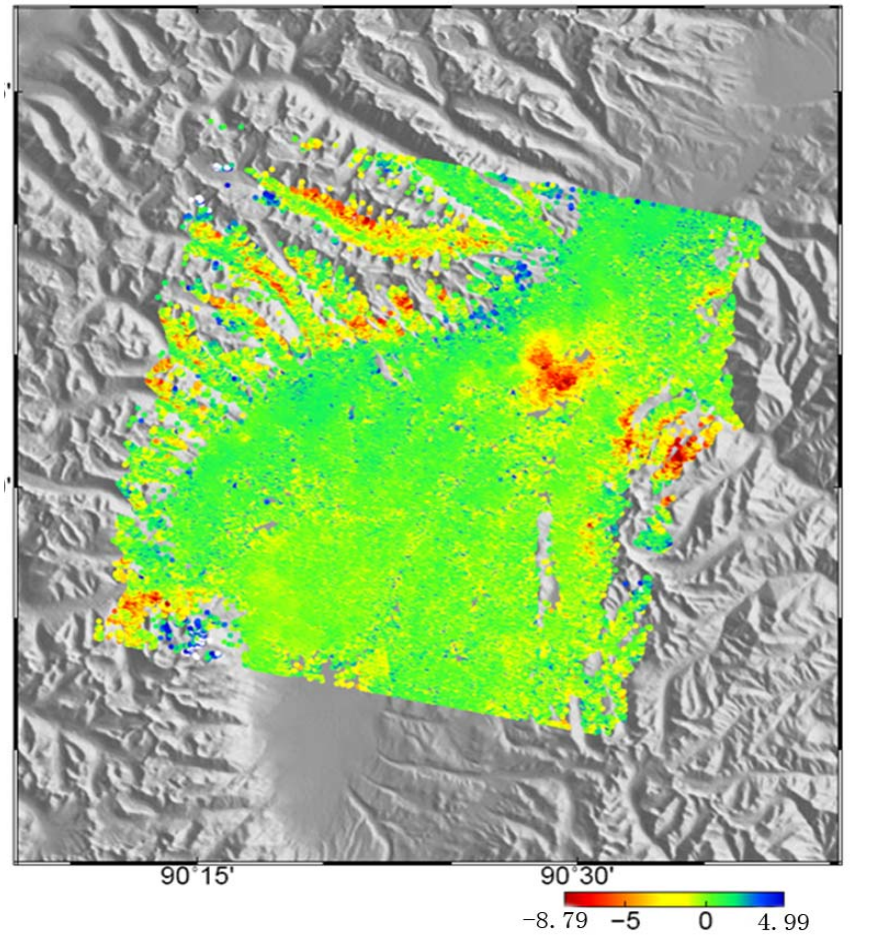

Time series analysis before the earthquake

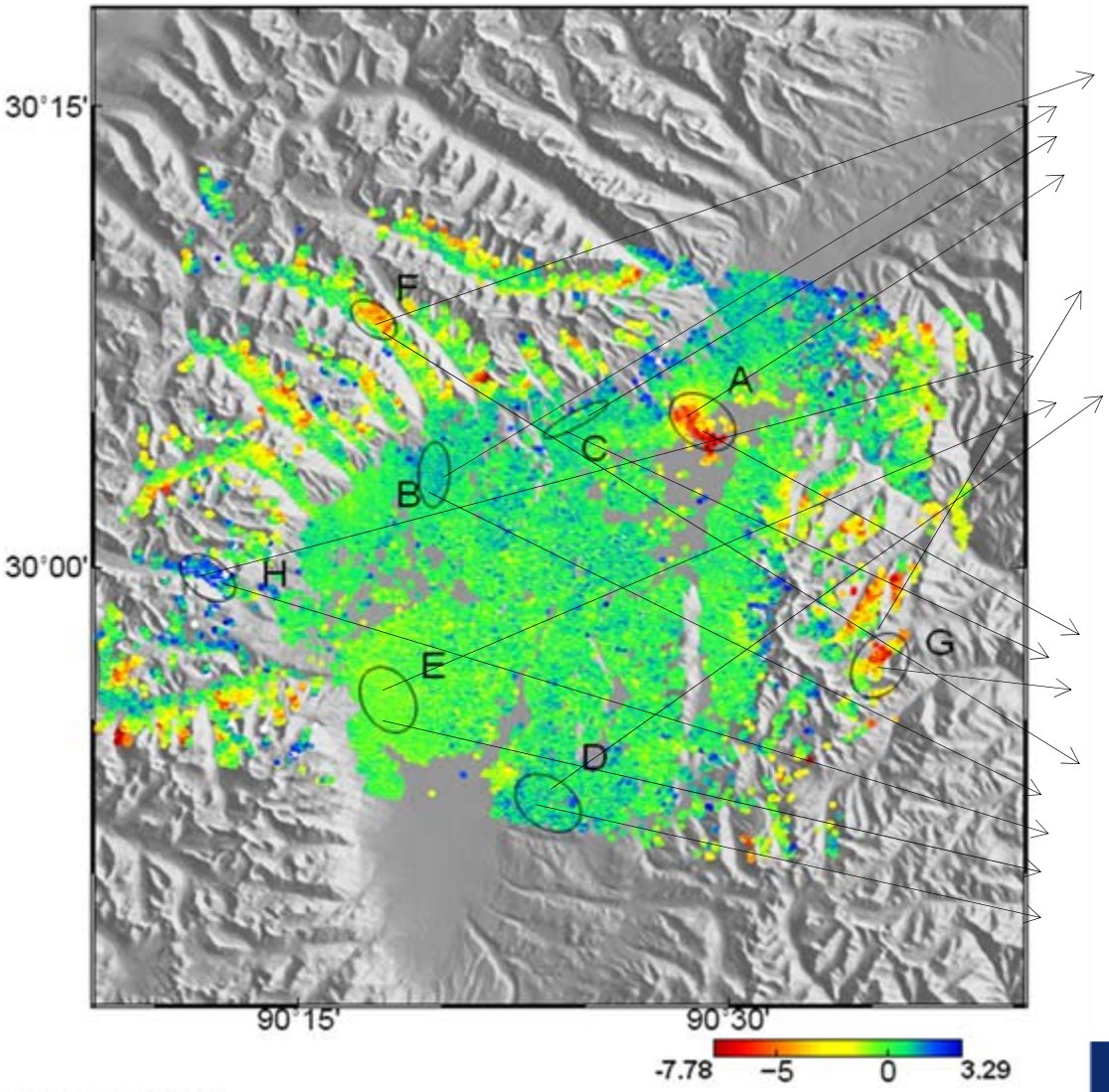

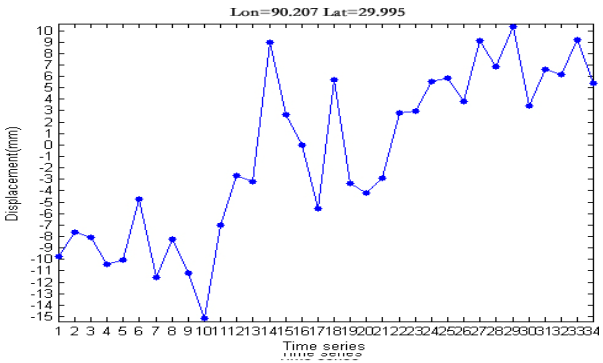

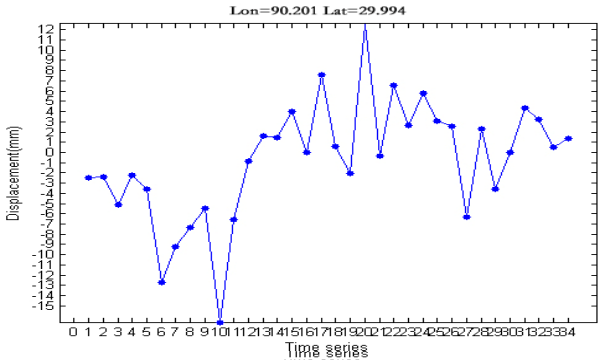

Time series analysis before the earthquake

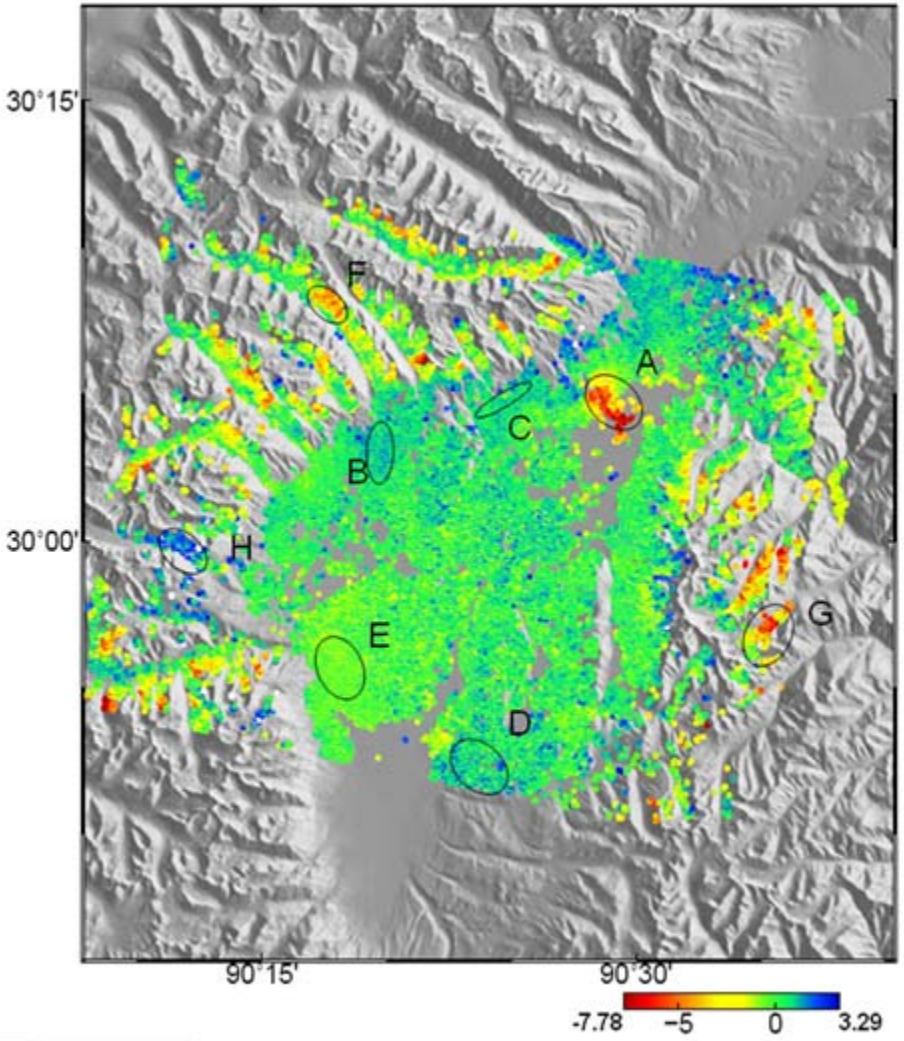

Standard deviations of the selected points in 8 areas

	Lon	Lat	mean_v (mm/year)	Std (mm/year)
区域 A	90.482	30.075	-6.74	0.61
	90.488	30.072	-7.78	0.76
区域 B	90.314	30.059	3.00	0.75
	90.310	30.059	2.33	0.69
区域 C	90.446	30.101	2.53	0.75
	90.464	30.121	3.30	0.72
区域 D	90.394	29.875	2.05	0.66
	90.384	29.887	1.63	0.53
区域 E	90.325	29.936	-1.04	0.49
	90.314	29.952	-1.73	0.45
区域 F	90.252	30.165	-3.82	1.62
	90.313	30.121	-1.92	1.15
区域 G	90.575	29.975	-4.21	1.5
	90.598	29.980	-3.93	1.44
区域 H	90.207	29.995	2.3	1.48
	90.201	29.994	3.16	1.48

Time series analysis before the earthquake

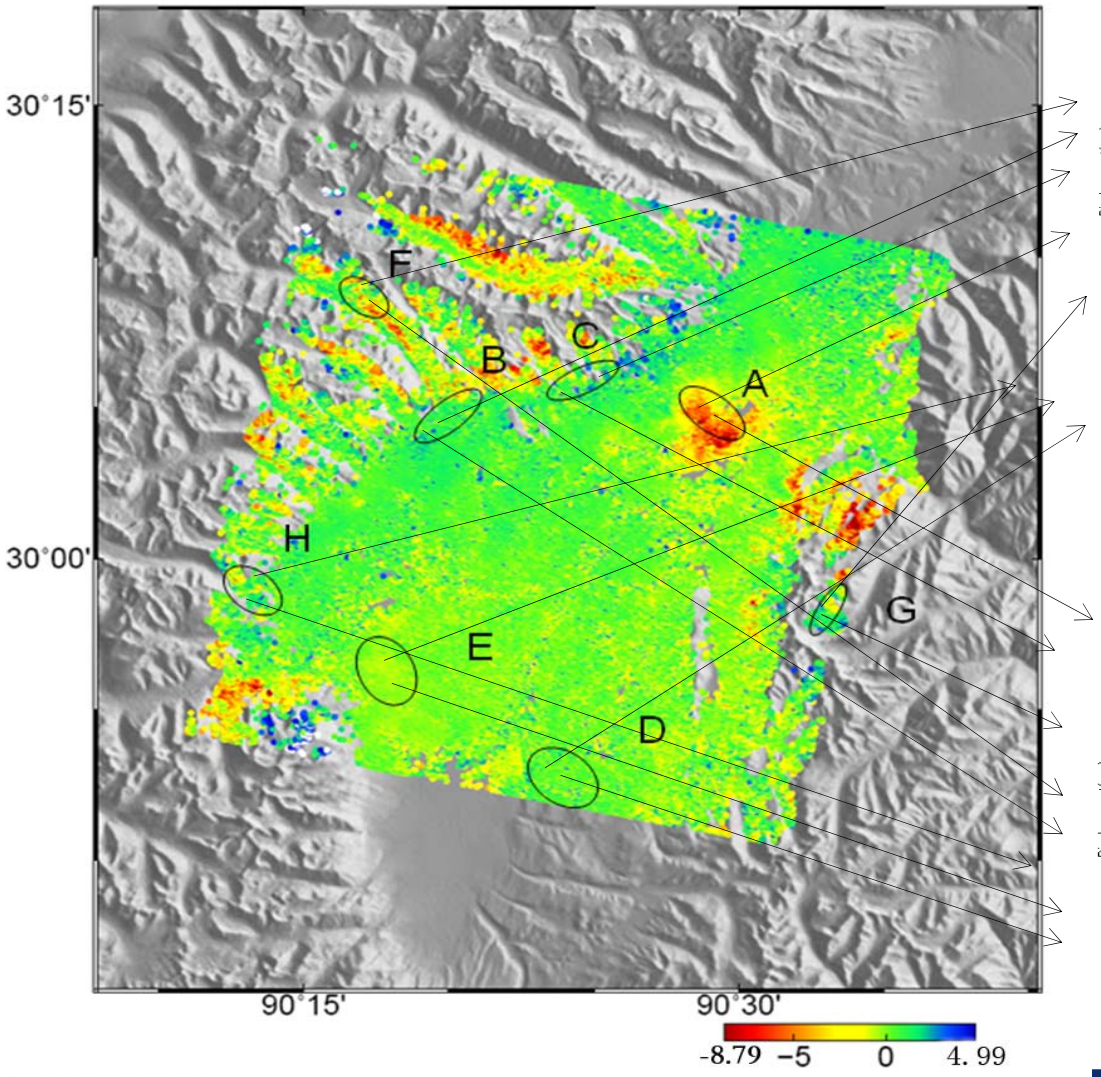

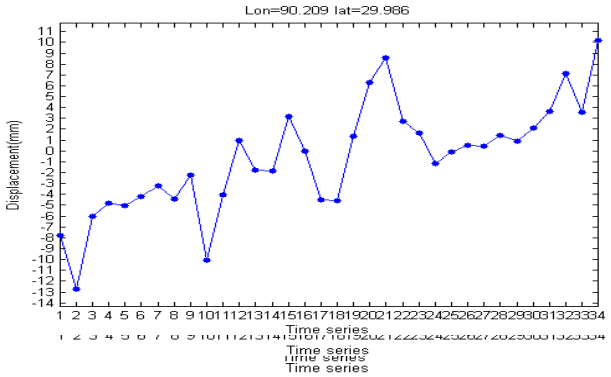

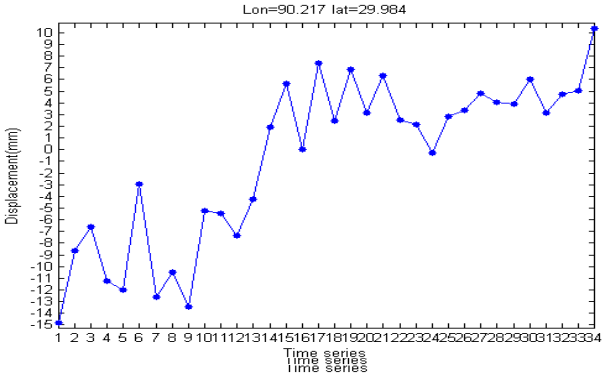

Time series analysis before the earthquake

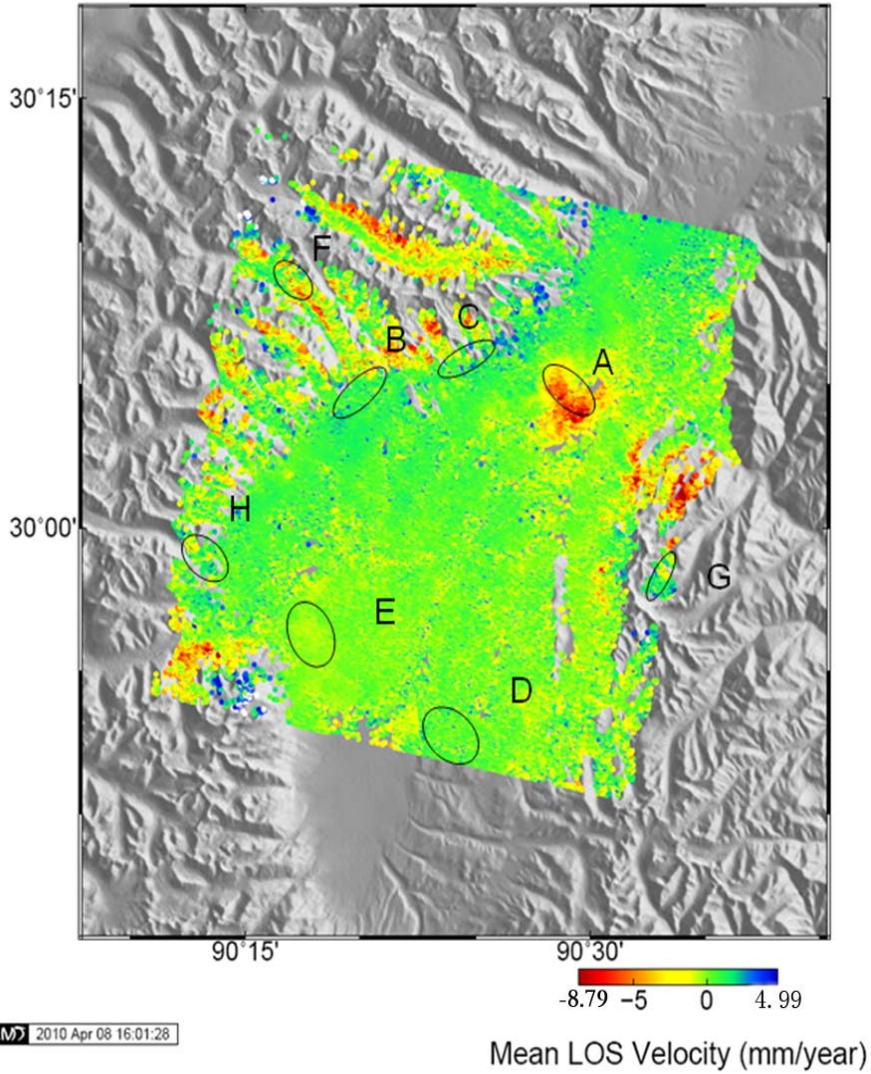

Standard deviations of the selected points in 8 areas

	Lon	Lat	mean_v (mm/year)	Std (mm/year)
区域 A	90.487	30.072	-7.20	0.62
	90.485	30.071	-7.23	0.65
区域 B	90.317	30.059	2.06	0.43
	90.317	30.06	2.28	0.29
区域 C	90.463	30.127	3.64	0.66
	90.464	30.125	3.15	0.54
区域 D	90.387	29.876	1.84	0.41
	90.381	29.881	2.21	0.45
区域 E	90.312	29.930	-1.11	0.33
	90.31	29.934	-0.98	0.32
区域 F	90.31	30.121	-6.08	0.6
	90.296	30.134	-5.93	0.82
区域 G	90.574	30.15	-4.21	0.86
	90.577	30.076	-2.07	0.78
区域 H	90.209	29.986	2.21	0.76
	90.217	29.984	3.68	0.85

Time series analysis before the earthquake

去噪后年形变速率（LOS）

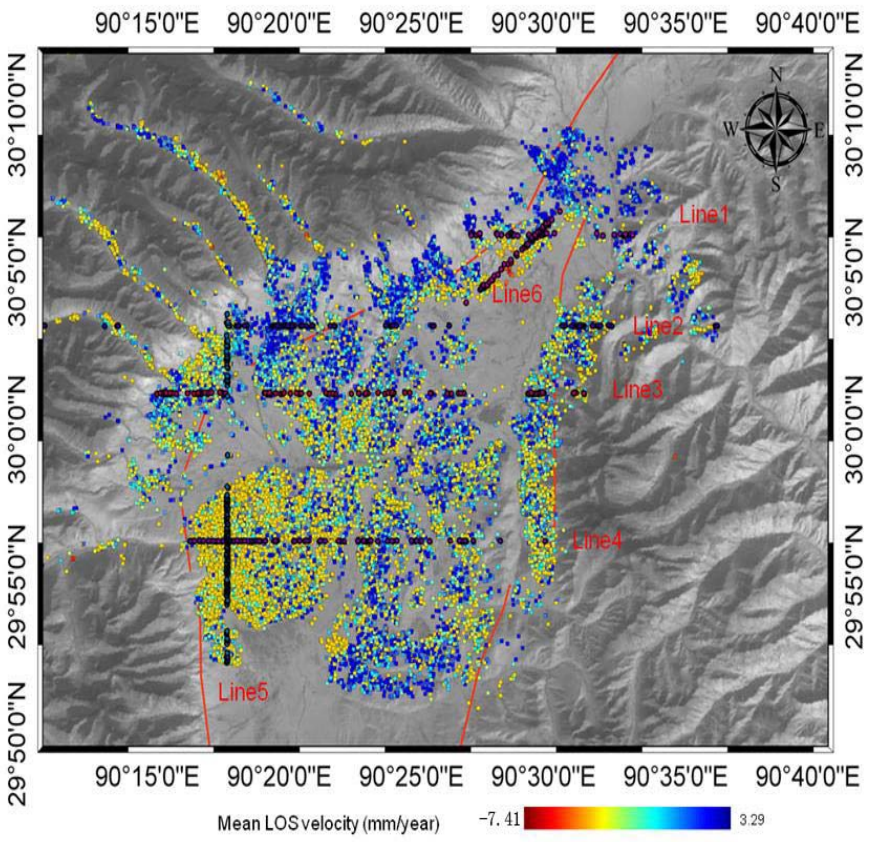

PS-meanv

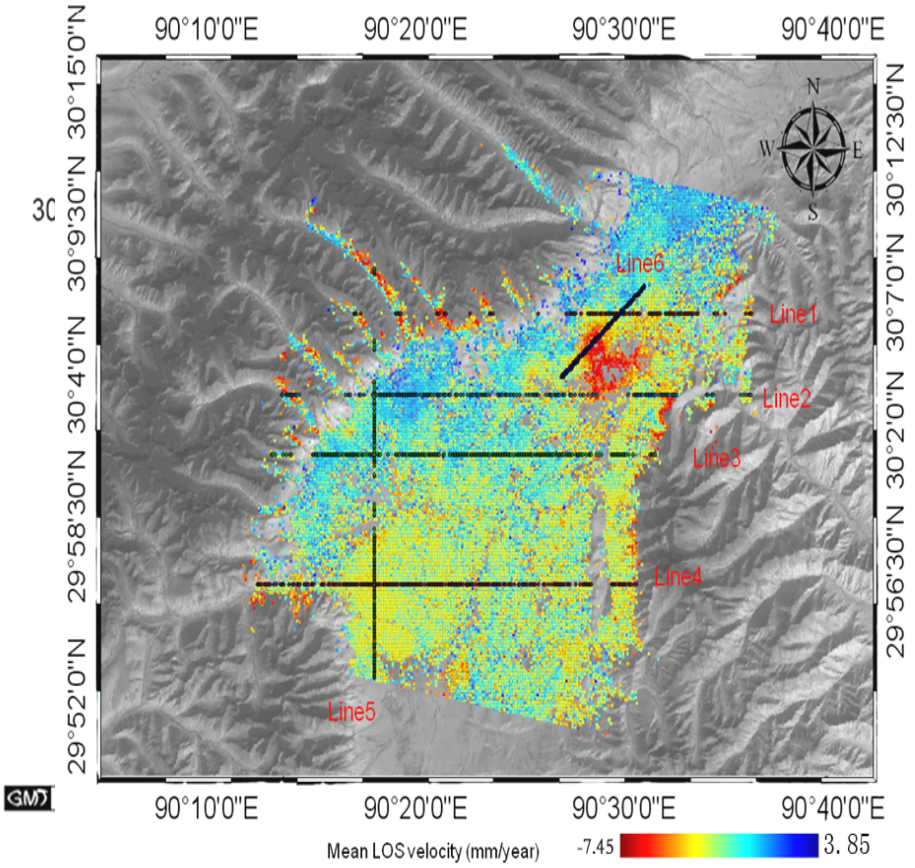

SBAS-meanv

Time series analysis before the earthquake

PS mean_v lines plot

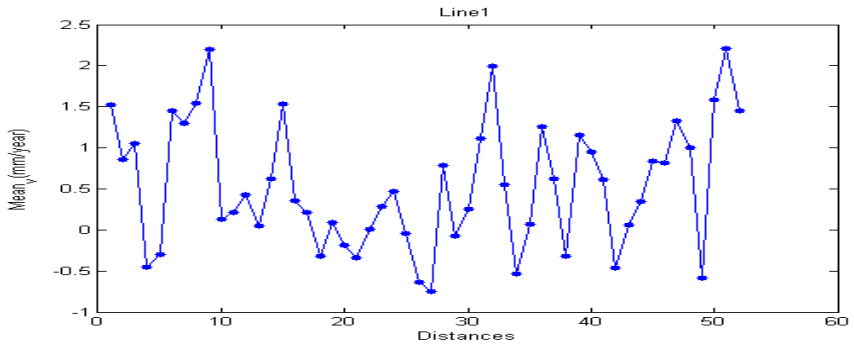

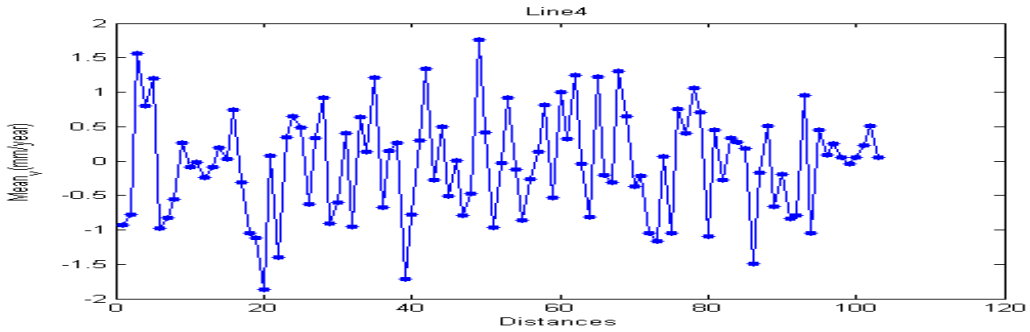

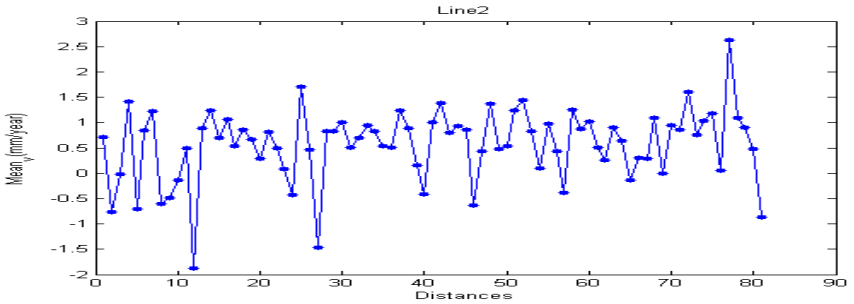

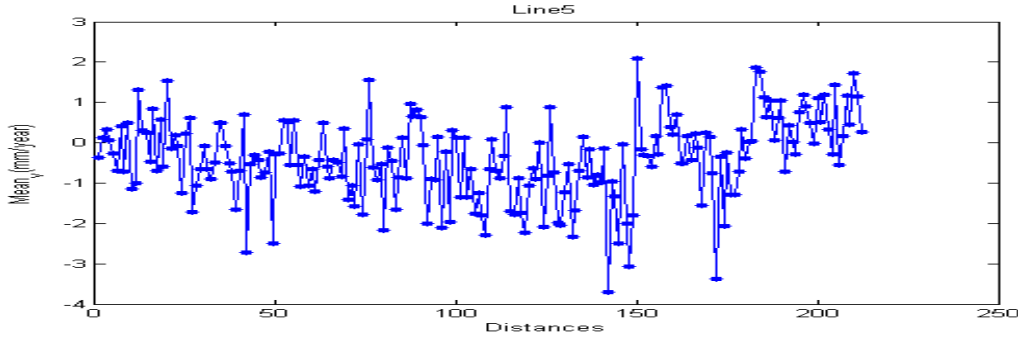

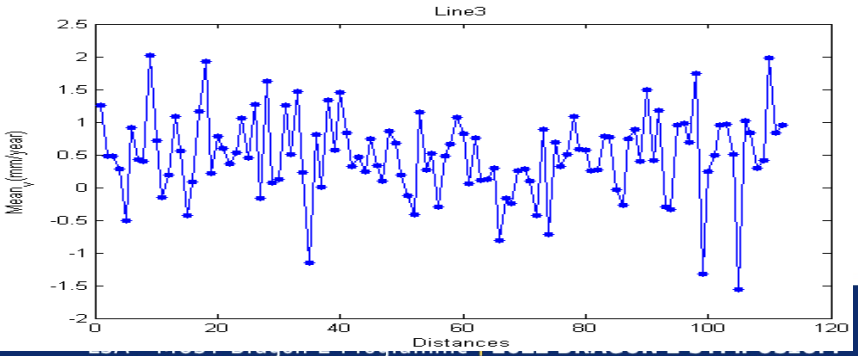

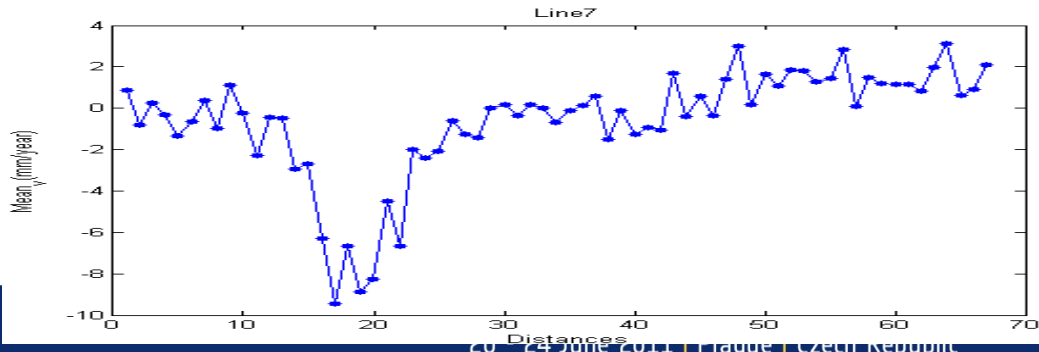

Time series analysis before the earthquake

SBAS mean_v lines plots

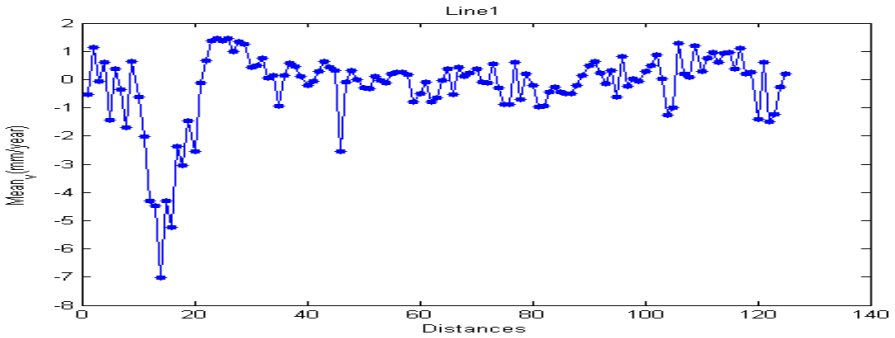

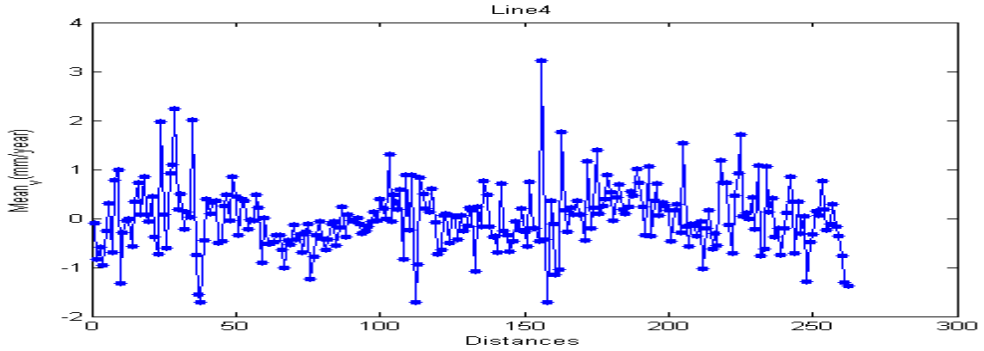

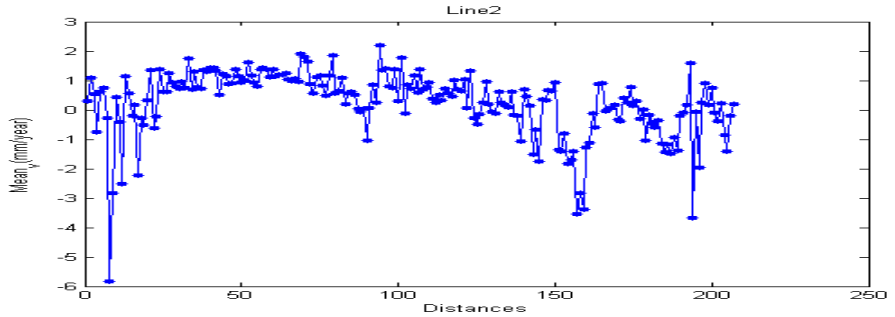

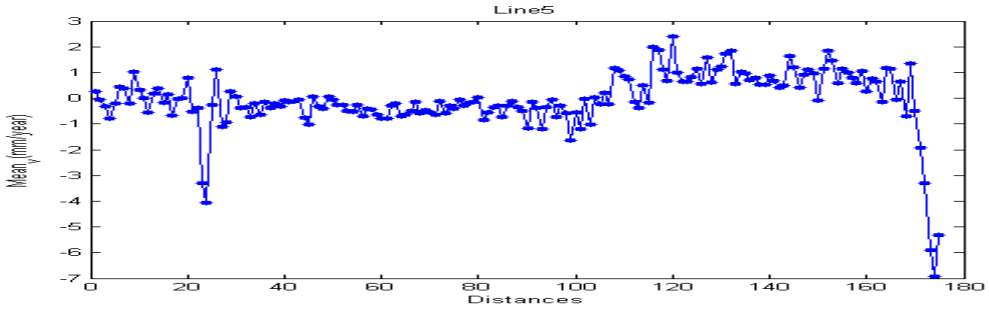

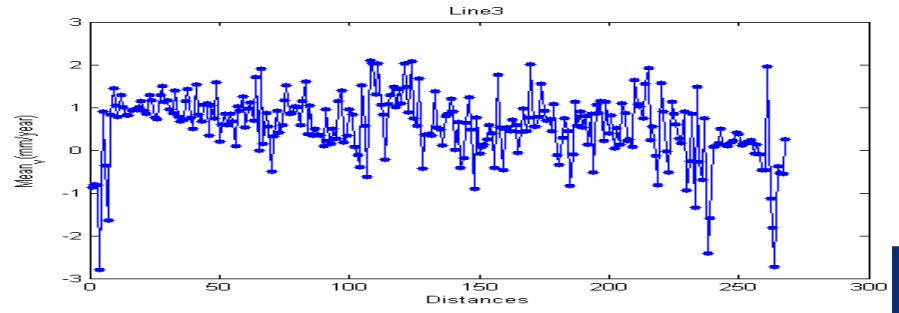

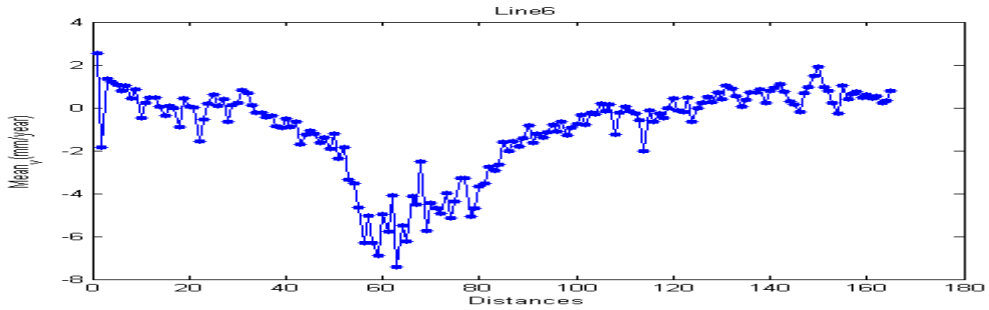

Time series analysis before the earthquake

The activities of faults in Yangbajing Basin

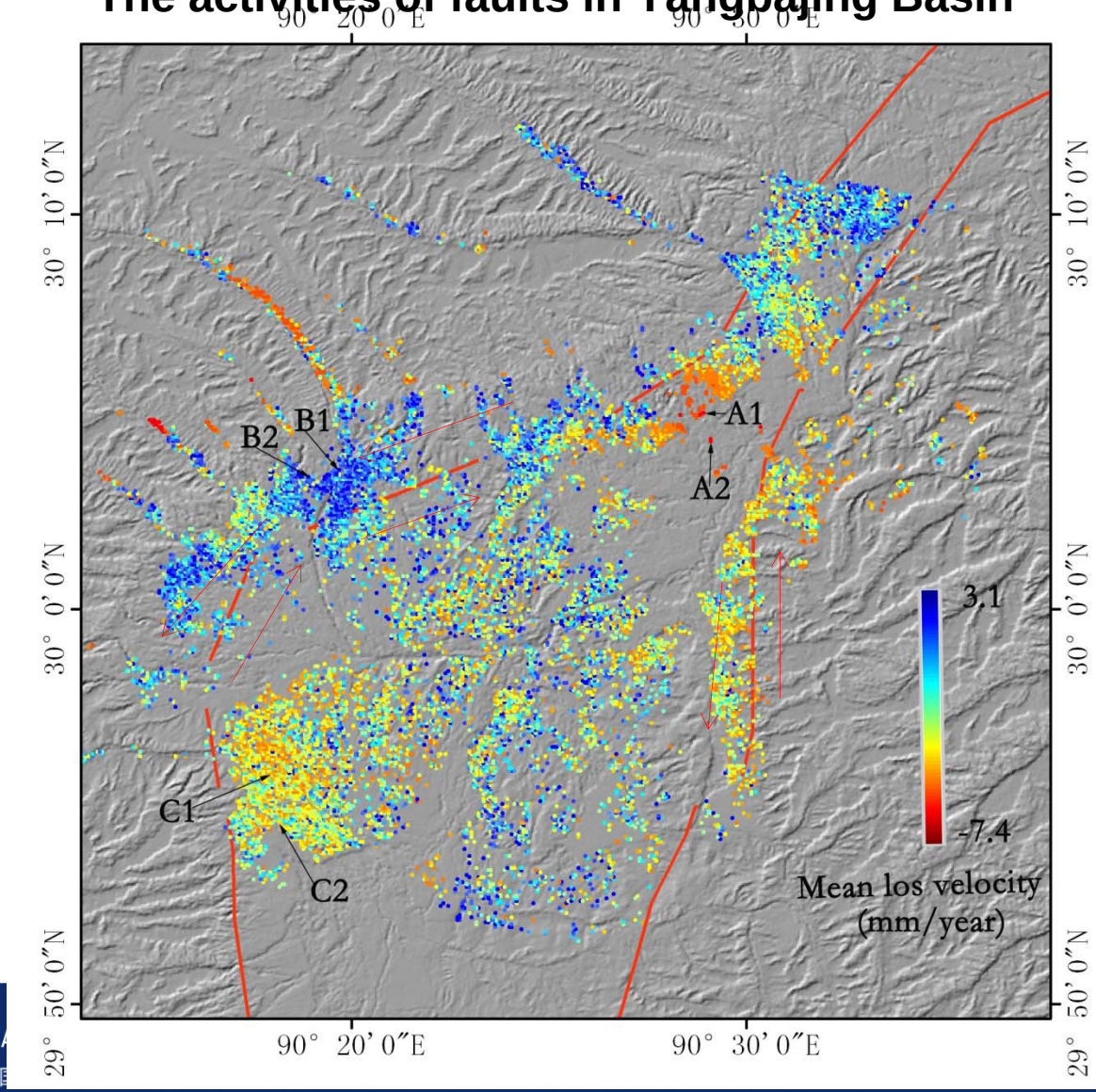

A: -5~-8mm/a

B：3~5mm/a

C:-1.5~2.0mm/a

After the Earthquake, from Oct. 26, 2008 to May 9, 2010，for Track 176, 13 scenes ASAR collected,

Aug. 2, 2009 as master

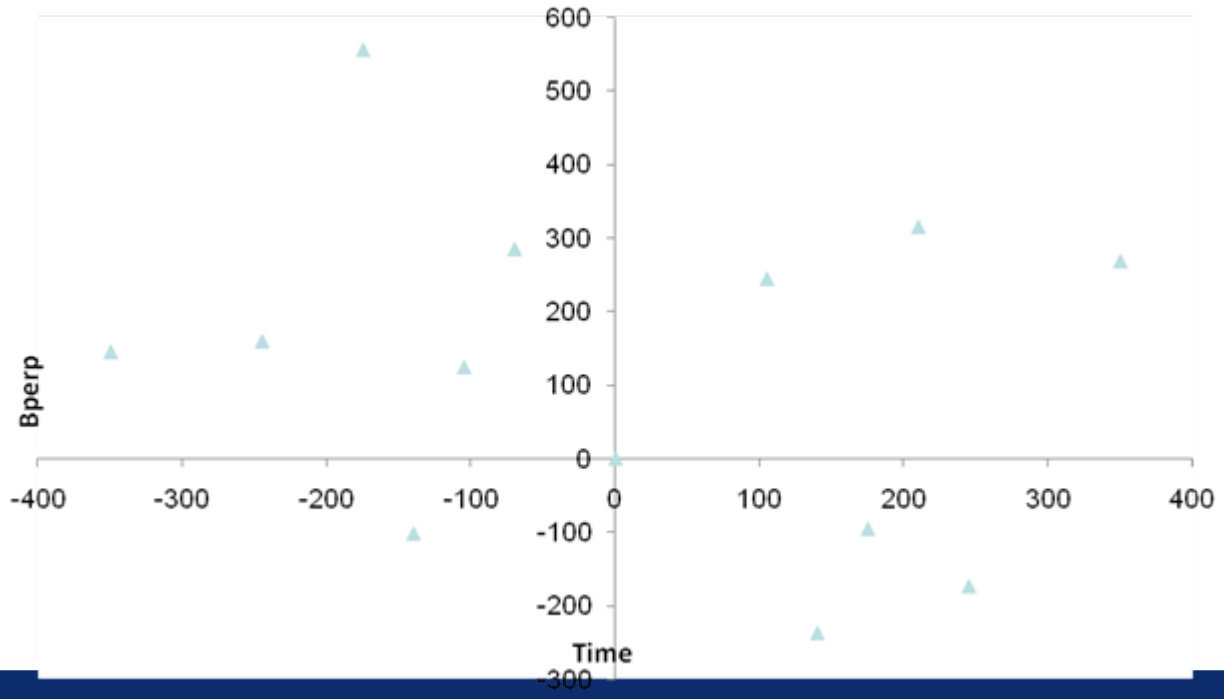

Time series analysis after the earthquake

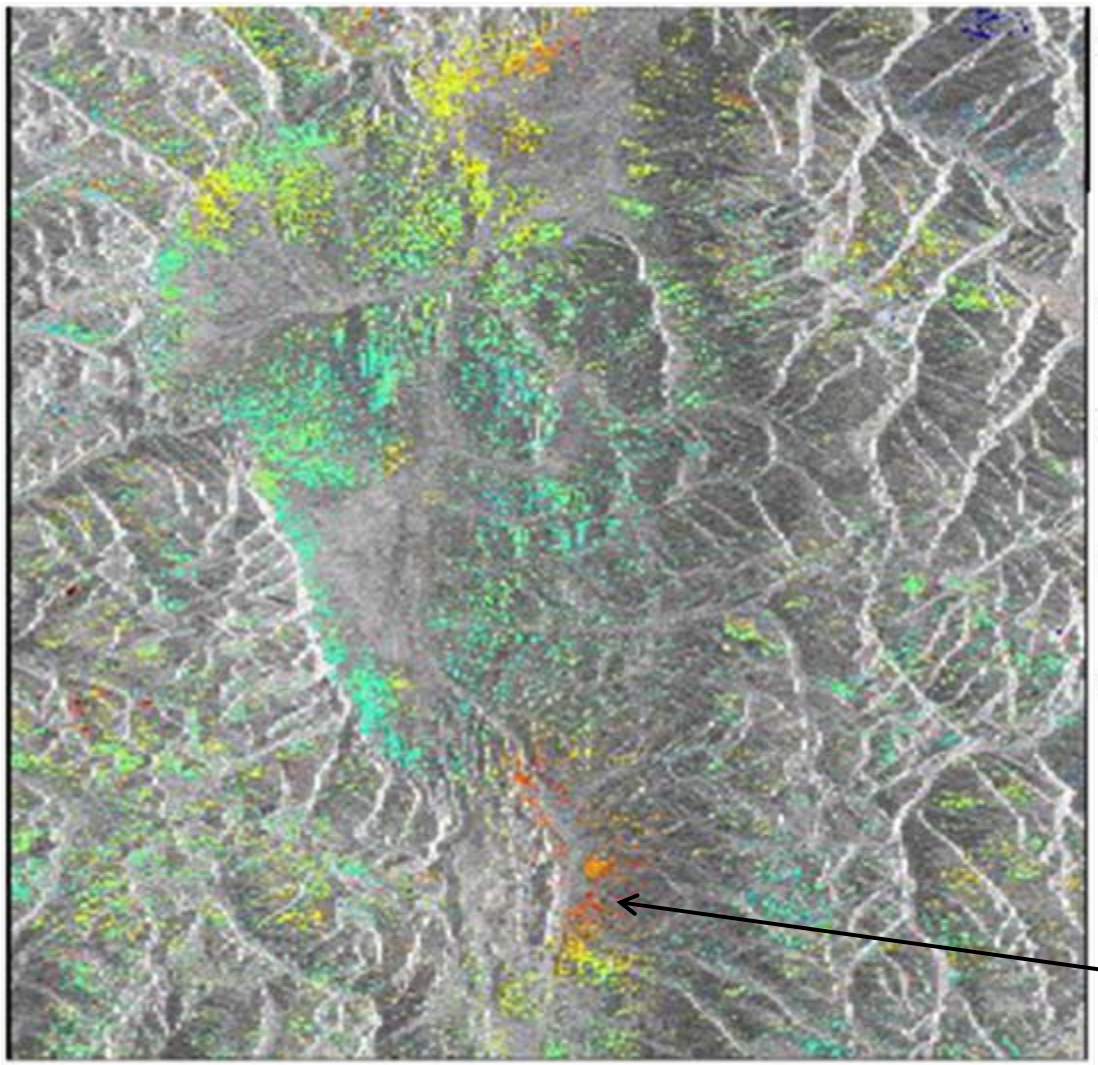

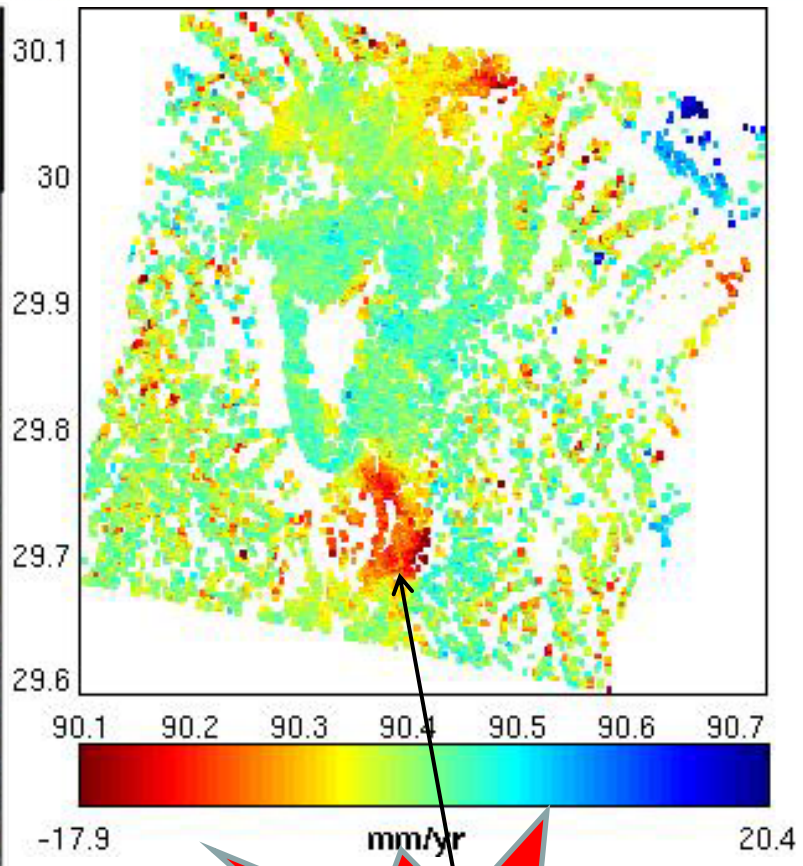

Damxung earthquake

Corner reflectors detection

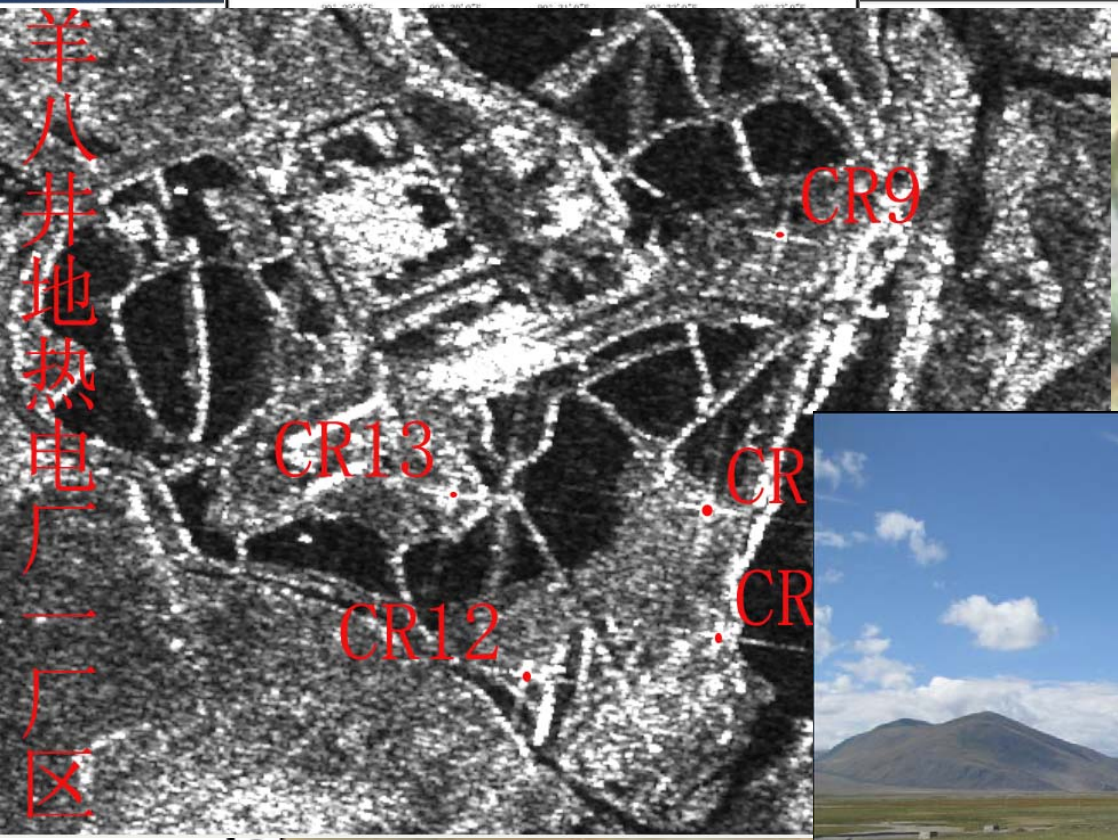

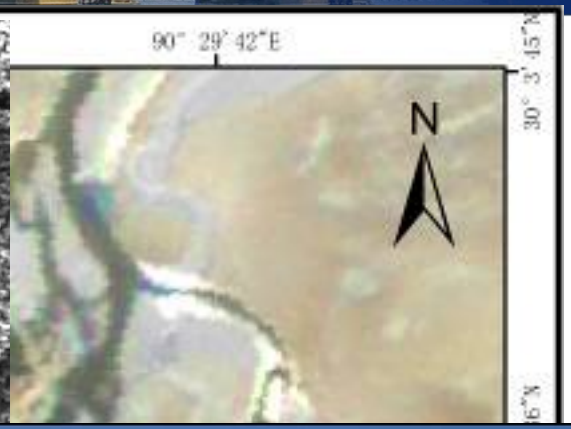

Corner reflectors detection

CR in the ASAR images, we filtered it and the
Corner reflectors are clear. It corresponds
to that inTerraSAR images.

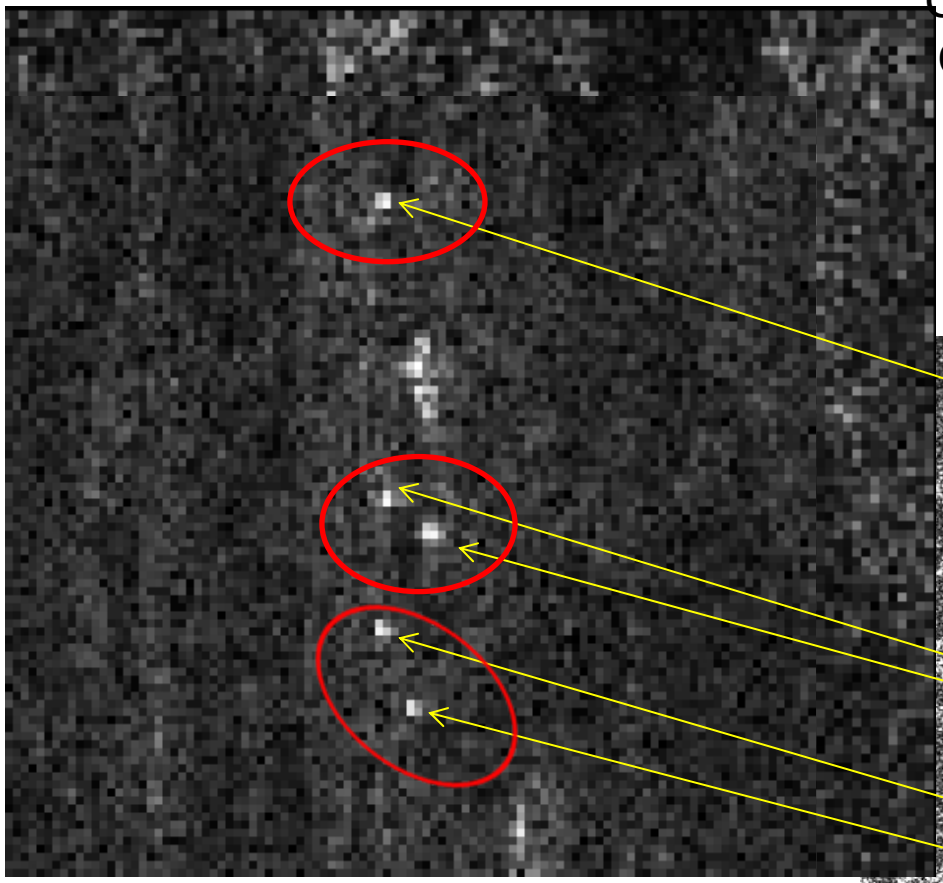

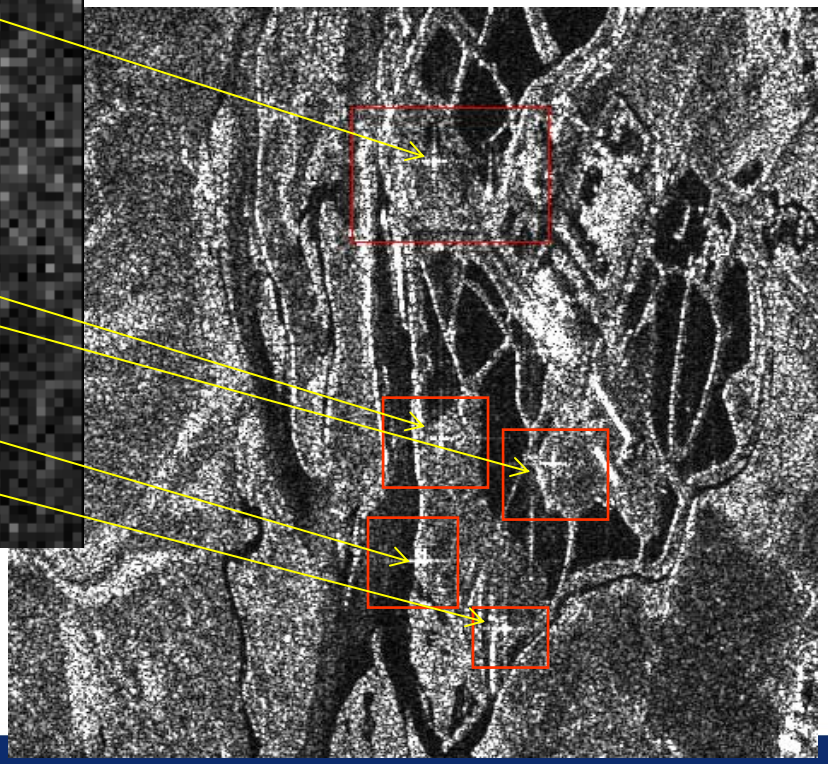

Corner reflectors detection

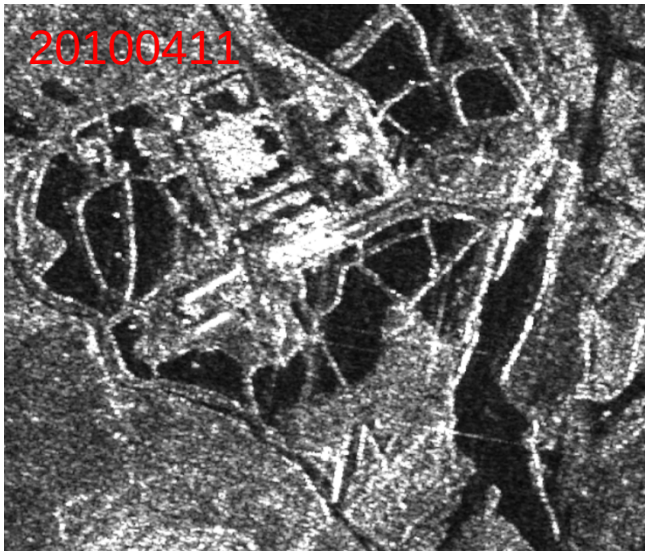

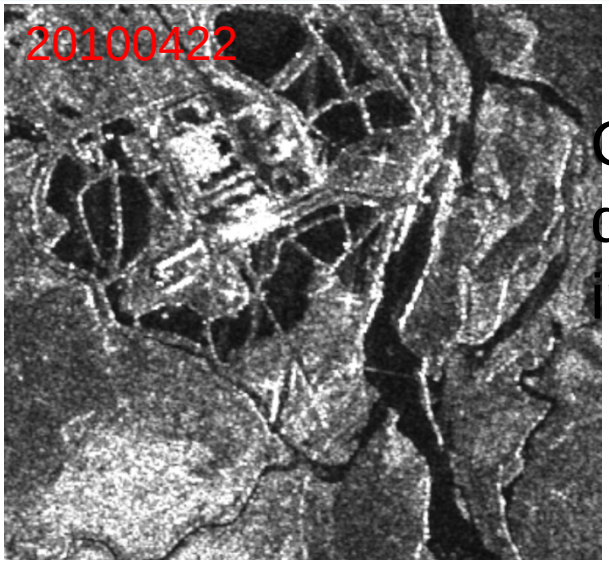

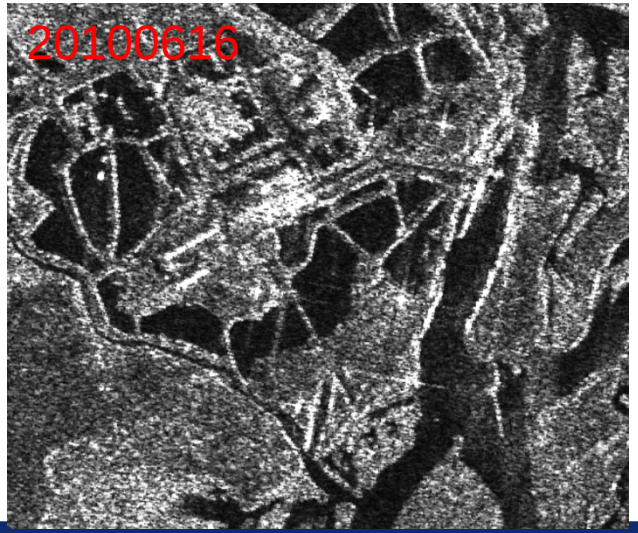

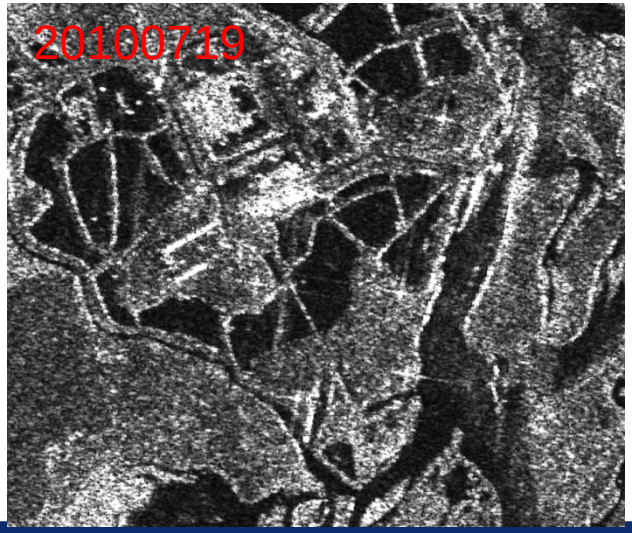

Corner reflectors in different TerraSAR images

OUTLINE

- Geological & Seismological Features
- Error Analysis & Deformation
- Numerical Simulation
- Conclusions

Numerical Simulation

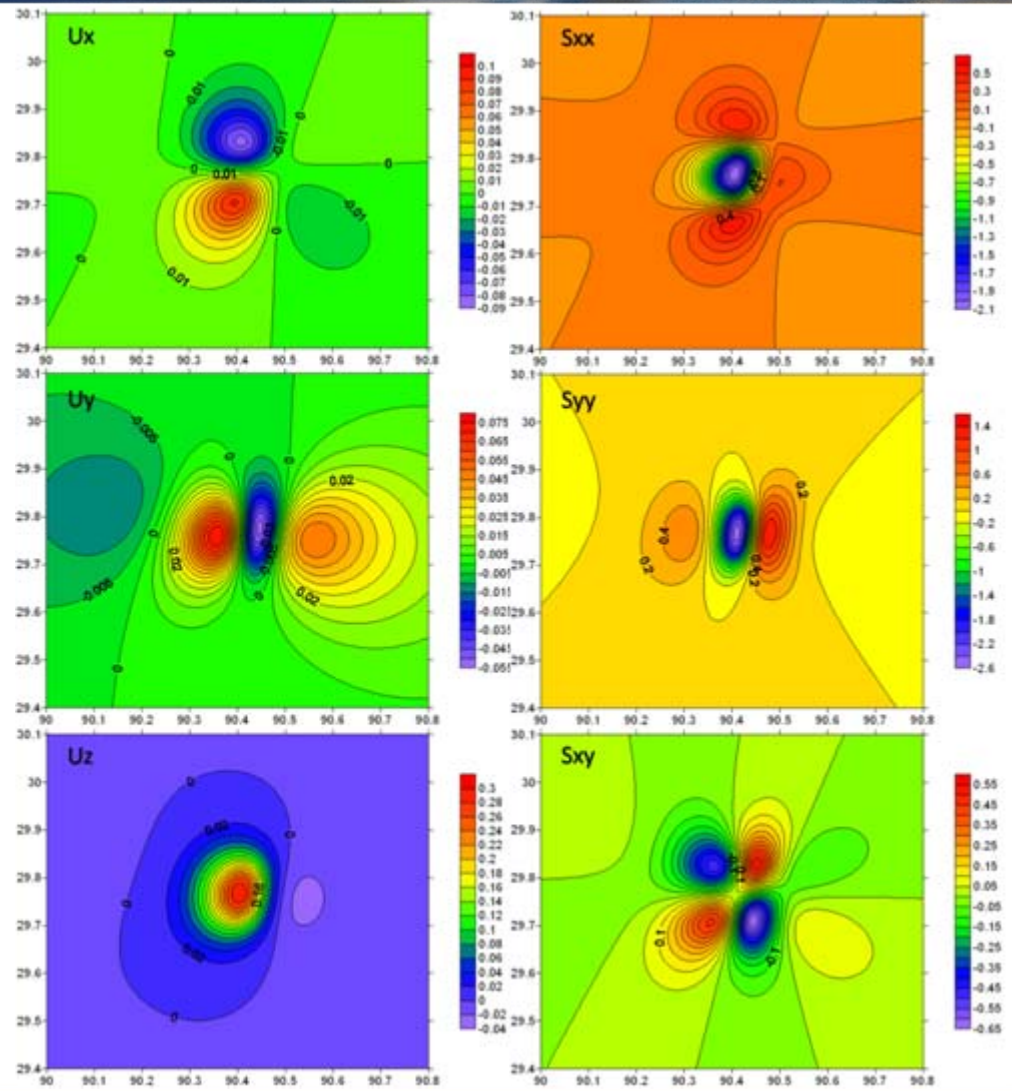

O_lat, O_lon, O_depth, length, width, strike, dip, slp_stk, slp_dip : 90.42, 29.64, 4.80, 12, 11, 188, 60, -0.5, 3.

Surface deformation and stress distribution
of the Dumxung earthquake
(Ux: deformation of NS; Uy: WE ;
Uz: vertical;
Sxx: normal stress of NS ;
Syy: WE;Sxy: shear)

Numerical Simulation

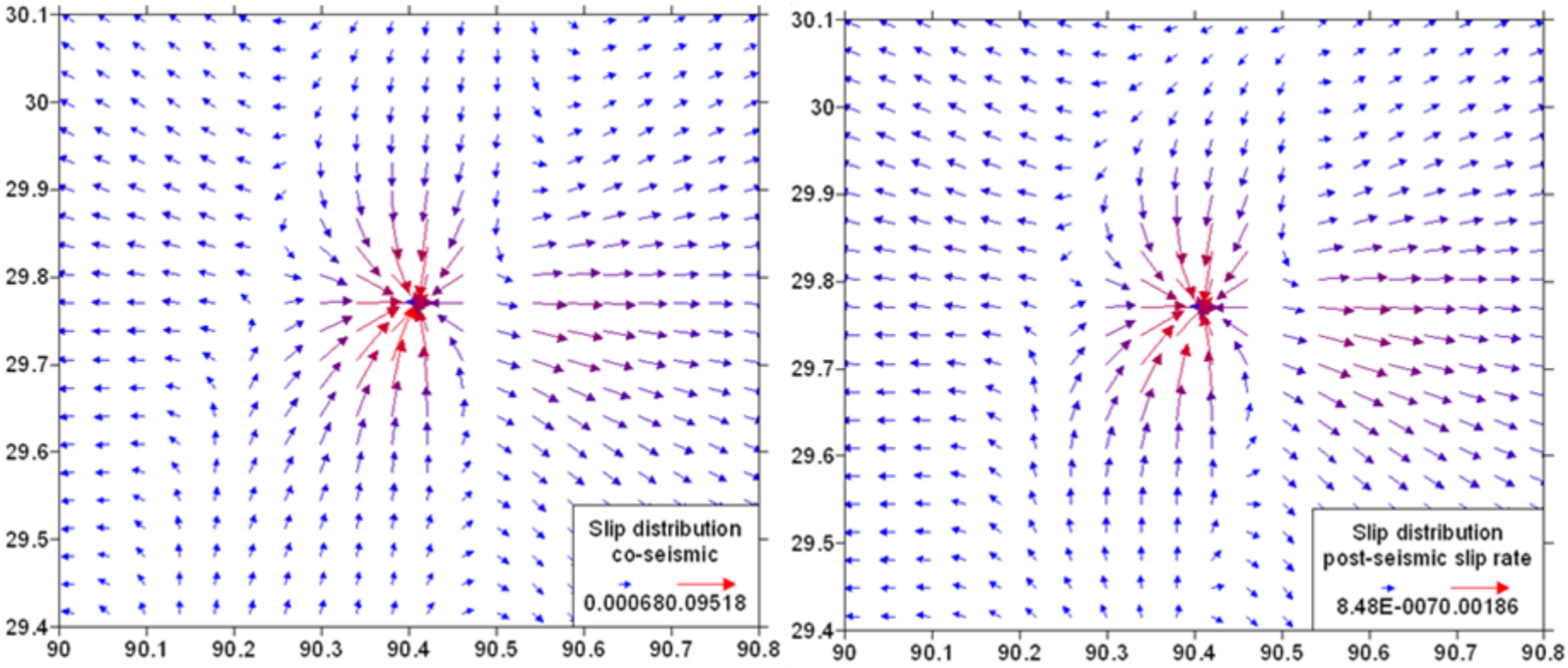

Horizontal surface displacement of Dumxung earthquake. Left: Vertical displacement of co-seismic deformation(mm); Right：Post-seismic deformation rate 50 years after the earthquake(mm/a)

Numerical Simulation

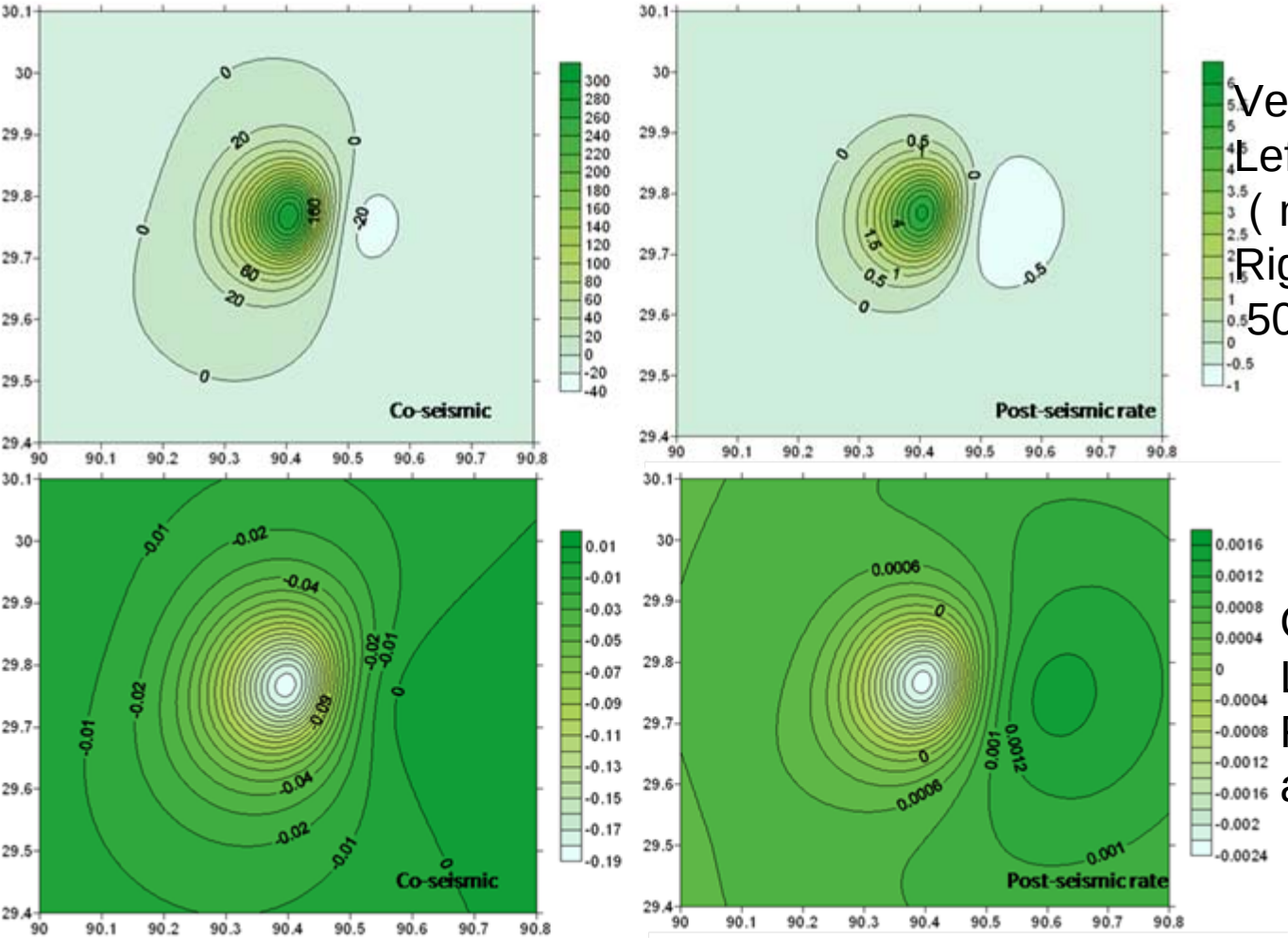

Vertical displacements.
Left: co-seismic deformation (mm) ;
Right: deformation rate after 50 years (mm/a)

Geoid changes
Left : co-seismic (mm)
Right: geoid change rate after 50 years (mm/a)

OUTLINE

- Geological & Seismological Features
- Error Analysis & Deformation
- Numerical Simulation
- Conclusions

Conclusions

1. The major perturbing factors limiting InSAR accuracy in deformation measurements is analyzed, such as coregistration between image to image and image to DEM, orbit contribution, atmospheric propagation and phase unwrapping errors. In Damxung earthquake, atmospheric contribution may be the largest error in measuring deformation.

Conclusions

2. InSAR time series analysis before and after the earthquake revealed that the velocity in the edge of the basin is bigger than the place in the flat area. Because of the impact of the aftershocks, in epicenter of Damxung, there is still ground subsidence in a long time after the earthquake.

Conclusions

3. Numerical simulation showes that the earthquake is dominated by oblique normal and a slightly right-lateral slip.

Thanks for your attention!